Air Pollution Science for the 21st Century
J. Austin, P. Brimblecombe and W. Sturges, editors

Chapter 21

Computation, accuracy and applications of trajectories—A review and bibliography

Andreas Stohl

Lehrstuhl für Bioklimatologie und Immissionsforschung, Ludwig-Maximilians-Universität München, Am Hochanger 13, D-85354 Freising-Weihenstephan, Germany

Abstract

To the authors knowledge, there exists no recent review paper on the computation and use of trajectories. To fill this gap, this study summarizes the current knowledge on the calculation and application of trajectories. The different techniques that can be used to compute trajectories are presented and their error sources are described. The assumptions often made to account for the vertical wind velocity are explained. Most studies agree now that fully three-dimensional trajectories are the most accurate trajectory type. Methods to assess trajectory errors are outlined and a summary of the errors presented in the literature is given. Errors of 20% of the distance travelled seem to be typical for trajectories computed from analyzed wind fields. Finally, some important applications of trajectories, namely Lagrangian particle dispersion models, Lagrangian chemical box models and trajectory statistics, are discussed.

1. Introduction

Trajectory models, which describe the paths air parcels take, have been used to study dynamical processes in the atmosphere for several decades now. Applications vary from synoptic meteorology, for instance to investigate airmass flow around mountains (Steinacker, 1984), to climatology, for instance to identify pathways of water vapor transport (D'Abreton and Tyson, 1996) or desert dust (Chiapello et al., 1997), to the environmental sciences, for instance to establish *source–receptor relationships* of air pollutants (Stohl, 1996a). They may be even used to detect illegal cultivation of marihuana by combining pollen measurements in the ambient air with back trajectories (Cabezudo et al., 1997).

Various methods to compute trajectories, based on different assumptions, have been developed, and the accuracy of calculated trajectories has improved

First published in Atmospheric Environment 32 (1998) 947–966

gradually since 1940 when Petterssen (1940) introduced a graphical technique to compute trajectories. In the literature, calculated trajectories are sometimes interpreted as if they represent "ground truth", but this is never the case. Trajectories are often highly uncertain, which can eventually lead to serious misinterpretations of a flow situation if the magnitude of the errors cannot be estimated (Kahl, 1993). One objective of this paper is to describe and compare the different methods developed to calculate trajectories, and to describe the data sources usually available for trajectory calculations. It will be discussed how accurate trajectories typically are, on what factors their accuracy depends, and how it can be estimated in individual situations. This is of fundamental importance, since the resolution at which source–receptor relationships can be established is limited by the accuracy of the trajectories (Pack et al., 1978).

Another topic of this paper is to discuss how trajectories are applied in the environmental sciences, beginning with a brief discussion on Lagrangian particle dispersion models (LPDM). LPDM are an interesting extension to conventional trajectory models, since they allow a more realistic representation of transport in the planetary boundary layer where turbulence is important.

It will be analyzed how trajectories can serve as an input to Lagrangian box models. Lagrangian box models are often used to simulate complex physical and chemical processes occurring in the atmosphere. These models are very popular because they pose smaller computational demands than Eulerian chemical transport models.

Several decades ago trajectories were only used to investigate the transport processes associated with individual air pollution events, but now there exist sophisticated methods based on large sets of trajectories, to study also the air pollution climatology of a site. These methods will be presented.

2. Computation of trajectories

2.1. Definition

There exist two different ways to view air motions, namely the *Eulerian* and the *Lagrangian* perspectives (Byers, 1974; Dutton, 1986). The first one focuses on points fixed in space through which the air flows, the second one on individual air parcels as they move through time and space. The paths of these air parcels are known as *trajectories.*

Let us assume that we have a specific infinitesimally small air parcel, then its trajectory is defined by the differential *trajectory equation*

$$\frac{\mathrm{d}\mathbf{X}}{\mathrm{d}t} = \dot{\mathbf{X}}[\mathbf{X}(t)] \tag{1}$$

with t being time, $\mathbf{X}$ the position vector and $\dot{\mathbf{X}}$ the wind velocity vector. If we know the initial position $\mathbf{X}_0$ at time t_0 of the parcel, its path is completely determined through Eq. (1). We can write

$$\mathbf{X}(t) = \mathbf{X}(\mathbf{X}_0, t). \tag{2}$$

We can also find the inverse transformation

$$\mathbf{X}_0(t = t_0) = \mathbf{X}_0(\mathbf{X}, t) \tag{3}$$

which gives the initial coordinates of the parcel, which at time t is at position $\mathbf{X}$. Thus, air parcels may be followed either forward (*forward trajectories*) or backward (*back trajectories*) in time. The spatial coordinates $\mathbf{X}_0$ at time t_0 provide a means of identifying each air parcel for all time. These initial coordinates are called *material* or *Lagrangian coordinates* (Dutton, 1986).

An important feature of trajectories is that particles that are initially neighbors remain neighbors for all time. A line of particles at time t_0 remains an unbroken line at time t, no matter how it is distorted by the motion. This can be expressed by

$$\lim_{\Delta X_0 \to 0} \left| \mathbf{X}(\mathbf{X}_0 + \Delta \mathbf{X}_0, t) - \mathbf{X}(\mathbf{X}_0, t) \right| = 0. \tag{4}$$

The most important property of Eq. (4) is that particles that are inside a closed surface at time t_0 are forever separated from those outside. The closed surface that moves with the flow is called a *material surface*. An interesting application of this feature is contour advection (Waugh and Plumb, 1994).

It has to be noted that trajectories are different from *streamlines*. A streamline represents the direction of flow at a fixed instant of time and thus is everywhere tangent to the velocity vectors. At a certain instant of time, each particle in the flow is moving along its trajectory and so the streamlines are parallel to the trajectories, but as time passes, the streamlines must adjust to the flow and trajectories and streamlines are no longer parallel. Only during *stationary conditions* are the trajectories and the streamlines the same.

The idealized concept discussed above is not fully applicable in the real atmosphere. With the limited information available, it is not possible to pick an infinitesimal air parcel and follow its path with infinite accuracy. A real parcel of finite size may become distorted so strongly in a divergent flow that it is torn apart. Pflüger et al. (1990) remark to this problem (from German): "Real air parcels of finite dimensions are drawn asunder and are being deformed by inhomogeneities of the wind field, by turbulent and convective motions and by precipitation processes. The combined action of these factors is the reason for the fact that in general a single trajectory is not sufficient for a description

of the path [of an air parcel] and that the mass center of gravity of the air parcel does not exactly follow the path of the computed trajectory." Hence, a computed trajectory is representative for the path of an air parcel only for a limited period.

2.2. Solution of the trajectory equation

Eq. (1) can be solved analytically only for simple flow fields; for meteorological applications, a finite-difference approximation of Eq. (1) must be used (Walmsley and Mailhot, 1983). Expanding $\mathbf{X}(t)$ in a Taylor series about $t = t_0$ and evaluating at $t_1 = t_0 + \Delta t$, one obtains

$$\mathbf{X}(t_1) = \mathbf{X}(t_0) + (\Delta t)\left.\frac{\mathrm{d}\mathbf{X}}{\mathrm{d}t}\right|_{t_0} + \frac{1}{2}(\Delta t)^2\left.\frac{\mathrm{d}^2\mathbf{X}}{\mathrm{d}t^2}\right|_{t_0} + \cdots. \tag{5}$$

The first approximation to Eq. (5) is

$$\mathbf{X}(t_1) \approx \mathbf{X}(t_0) + (\Delta t)\dot{\mathbf{X}}(t_0) \tag{6}$$

a "*zero acceleration*" *solution* of Eq. (1) that is computationally cheap since it involves no iteration. It is accurate to the first order, which means that differences between the real and the numerical solution occur from the ommision of the second- and higher-order terms. If trajectories are calculated using very short integration time steps, Eq. (6) might be of sufficient accuracy. However, more accurate approximations at acceptable computational costs exist. If $\mathbf{X}(t)$ is also expanded in a Taylor series about $t = t_1$ and evaluated a $t = t_0$, this yields:

$$\mathbf{X}(t_0) = \mathbf{X}(t_1) - (\Delta t)\left.\frac{\mathrm{d}\mathbf{X}}{\mathrm{d}t}\right|_{t_1} + \frac{1}{2}(\Delta t)^2\left.\frac{\mathrm{d}^2\mathbf{X}}{\mathrm{d}t^2}\right|_{t_1} - \cdots. \tag{7}$$

Combining Eqs. (5) and (7), we obtain

$$\mathbf{X}(t_1) = \mathbf{X}(t_0) + \frac{1}{2}(\Delta t)\left[\dot{\mathbf{X}}(t_0) + \dot{\mathbf{X}}(t_1)\right] + \frac{1}{4}(\Delta t)^2\left[\left.\frac{\mathrm{d}\dot{\mathbf{X}}}{\mathrm{d}t}\right|_{t_0} - \left.\frac{\mathrm{d}\dot{\mathbf{X}}}{\mathrm{d}t}\right|_{t_1}\right] + \cdots. \tag{8}$$

If only the first two terms on the right-hand side of Eq. (8) are retained, the "*constant acceleration*" *solution*

$$\mathbf{X}(t_1) \approx \mathbf{X}(t_0) + \frac{1}{2}(\Delta t)\left[\dot{\mathbf{X}}(t_0) + \dot{\mathbf{X}}(t_1)\right] \tag{9}$$

results (Walmsley and Mailhot, 1983). This approximation is identical to Petterssen's (1940) scheme, originally a graphical method to construct isobaric trajectories manually from weather charts. Eq. (9) is accurate to the second order. It has to be solved by iteration starting with Eq. (6), since $\dot{\mathbf{X}}(t_1)$ is not *a priori* known:

$$\begin{aligned}
\mathbf{X}^1(t_1) &\approx \mathbf{X}(t_0) + (\Delta t)\dot{\mathbf{X}}(t_0) \\
\mathbf{X}^2(t_1) &\approx \mathbf{X}(t_0) + \frac{1}{2}(\Delta t)\left[\dot{\mathbf{X}}(t_0) + \dot{\mathbf{X}}^1(t_1)\right] \\
&\vdots \\
\mathbf{X}^i(t_1) &\approx \mathbf{X}(t_0) + \frac{1}{2}(\Delta t)\left[\dot{\mathbf{X}}(t_0) + \dot{\mathbf{X}}^{i-1}(t_1)\right]. \qquad (10)
\end{aligned}$$

The superscripts indicate the number of iteration, and $\dot{\mathbf{X}}^i(t_1)$ is taken at position $\mathbf{X}^i(t_1)$.

Sometimes, the third term on the right-hand side of Eq. (8) is retained, too (*"variable acceleration" method*). In principle, this solution gives higher accuracy at the cost of increased computing time, but it has the disadvantage that the accelerations at two times must be evaluated. This can be inaccurate because wind fields are often available only at large temporal intervals. Hence, the variable acceleration method may even be less accurate than the constant acceleration method. If linear interpolation of the wind is used, the third term on the right-hand side of Eq. (8) vanishes, and the "variable acceleration" method reduces to the "constant acceleration" method.

All solutions discussed sofar are *kinematic* because they use the wind information only. Danielsen (1961) developed a technique to construct trajectories by tagging air parcels with (*quasi-*) *conservative quantities* such as potential temperature. Although two-dimensional kinematic trajectories can also be constructed on isentropic surfaces, Danielsen's (1961) method is *dynamic* because it makes use of velocity *and* mass field information and of *dynamic equations* linking the two (Merrill et al., 1986). Various different dynamic methods have appeared in the literature. The one of Petersen and Uccellini (1979) is based on the integration of the equation of motion for inviscid, adiabatic flow in isentropic coordinates,

$$\frac{\mathrm{d}\mathbf{v}_\mathrm{h}}{\mathrm{d}t} + \nabla_\Theta M + f\,\mathbf{k} \times \mathbf{v}_\mathrm{h} = 0, \qquad (11)$$

where $\mathbf{v}_\mathrm{h}$ represents the horizontal wind vector, ∇_Θ is the gradient on isentropic surfaces, $M = c_p T + gz$ is the Montgomery potential, with c_p being the heat capacity of air at constant pressure, T the temperature and gz the geopotential, and f the Coriolis parameter. Using an estimation for the wind at the

starting position and integrating Eq. (11), this method produces wind vectors along a trajectory.

For some time, dynamic methods were very popular (Merrill et al., 1986; Steinacker, 1984) because they allowed to use long intervals between the wind fields. For instance, Merrill et al. (1986) found that dynamic and two-dimensional kinematic trajectories calculated on isentropic surfaces agree very well for short intervals between the wind fields, but that dynamic trajectories calculated either with the implicit technique of Danielsen (1961) or with the explicit technique of Petersen and Uccellini (1979) are superior for wind field intervals in excess of 3 h. However, Stohl and Seibert (1997) showed that dynamic trajectories calculated with Steinacker's (1984) explicit method can perform unrealistic ageostrophic oscillations at travel times longer than 24 to 48 h that result from inaccurate determination of M. Since nowadays accurate wind fields with high space and time resolution are available, kinematic trajectories are more accurate (Stohl and Seibert, 1997).

2.3. Data sources for the computation of trajectories

In principle, trajectories can be calculated directly from wind observations by interpolating between the measurement locations. In practice, however, trajectory calculations are mostly based on the gridded output of numerical models. The most simple models are *diagnostic wind field models* (Sherman, 1978; Goodin et al., 1980; Ross et al., 1988; Mathur and Peters, 1990; Scire et al., 1990; Ludwig et al., 1991), some doing little more than interpolating radiosonde measurements, and adjusting them to fulfill mass consistency. Although their grid spacing may be much smaller than the average distance between radiosondes, due to a lack of model physics their effective resolution at upper levels is often limited by the resolution of the radiosonde network. Hence, there may be not much difference to interpolating directly from the measurement locations. If a dense network of surface wind measurements exists, the downscaling technique of Stohl et al. (1997) can yield more accurate wind fields in the planetary boundary layer (PBL) than conventional diagnostic models, but its applicability may be restricted to rather simple terrain.

On the synoptic scale, the most accurate wind data come from *numerical weather prediction* (NWP) centers. They use the most sophisticated methods currently available to produce accurate analysis fields to start their model forecasts. Hence a time series of these analyses should be used whenever possible. An additional bonus of this data source is that the data are easily accessible to many researchers. From most NWP models, data are available either on levels used internally by the model or on pressure levels that are interpolated from the model levels for synoptic purposes. For trajectory calculations, data on model levels are clearly better suited since interpolation errors are much smaller.

On the mesoscale, *prognostic mesoscale models* may produce more accurate wind fields (Pielke et al., 1992; Grell et al., 1995; Schlünzen, 1994). This requires, however, a very sophisticated and well validated modeling system. Important criteria that should be considered when the output of a mesoscale model is selected as the basis of trajectory computations are:

- Is the model physics suitable for the scale considered, for instance is the model non-hydrostatic?
- Is the terrain resolution sufficient?
- Is the soil moisture specified adequately?
- Are the data used for model initialization and for boundary conditions of high quality?
- Are four-dimensional data assimilation techniques used to improve the forecast or to develop a better analysis archive?

Only modeling systems that are carefully selected according to the above and many other criteria can reproduce real small-scale structures in the wind fields. Otherwise, the wind fields, although containing much variation, may actually be less accurate than those of NWP models or those derived from radiosonde measurements.

2.4. Error sources for the computation of trajectories

Before discussing error sources, it is necessary to describe how differences between trajectories can be measured. Assessment of trajectory errors is often done in a statistical framework. Unfortunately, there exists some confusion in the literature regarding the statistical parameters used. Sometimes the same names have been given to different parameters, or different names have been given to identical ones. A measure that has been adopted by many authors in recent years is the absolute horizontal transport deviation (Kuo et al., 1985; Rolph and Draxler, 1990)

$$\mathrm{AHTD}(t) = \frac{1}{N}\sum_{n=1}^{N}\left\{\left[X_n(t) - x_n(t)\right]^2 + \left[Y_n(t) - y_n(t)\right]^2\right\}^{1/2}, \qquad (12)$$

where N is the number of trajectories used, X and Y are the locations of the test trajectories and x and y are the locations of some reference trajectories at travel time t. A similar measure can be defined in the vertical.

Another parameter often used is the relative horizontal transport deviation (RHTD). However, there exist several different definitions of RHTD. Some authors define RHTD as the AHTD divided by the average length of the reference trajectories (e.g. Rolph and Draxler, 1990), while others divide by the average

length of test and reference trajectories (e.g. Stohl et al., 1995). In addition, the length of the trajectories is sometimes defined as the straight-line distance between the starting and ending points (e.g. Kuo et al., 1985), and sometimes as the length of the curved trajectory (e.g. Rolph and Draxler, 1990; Stohl et al., 1995). Currently, no general suggestion can be made regarding which of these definitions should be used in future work, but it is important to keep these differences in mind when comparing relative errors from different studies. Several other measures, like directional deviations, differences in length or in meandering, etc., have also been used, but it seems advisable to report them only in addition to AHTD and RHTD since they cannot be compared as readily with results of other authors.

Once large trajectory errors have occurred, trajectories separate further not only due to the occurrence of additional errors, but also due to the wind shear. An anonymous reviewer of the original version of this paper commented to this fact: "It hardly seems important to compare trajectories after they have separated some distance and are in different flow regimes—after which the errors will just amplify. It seems we need some type of approach that measures the length scale of the flow in which the trajectory is calculated. Once the error exceeds the length scale any further statistics are meaningless." Unfortunately, no such length scale has been used yet.

2.4.1. Truncation errors

The so-called *truncation errors* result when Eq. (1) is approximated by a finite-difference scheme that neglects the higher order terms of the Taylor series. Walmsley and Mailhot (1983) showed that the truncation error is proportional to Δt for the zero [Eq. (6)] and proportional to $(\Delta t)^2$ for the constant [Eq. (9)] and variable acceleration method. It can be kept below any desired limit by using sufficiently small Δt.

Walmsley and Mailhot (1983) computed trajectories with a numerical scheme of high order using very short time steps to keep truncation errors negligible. They compared these "exact" trajectories with ones computed with the operational methods discussed above using time steps of 3 h. After 42 h, position errors of the trajectories were 300 km for the zero acceleration, 100 km for the constant acceleration and 40 km for the variable acceleration method. Since an error of 300 km is significant when compared to other errors, the zero acceleration method can only be used with time steps much shorter than 3 h.

Similar results were obtained by Seibert (1993) who compared analytical solutions of the trajectory equation with numerical solutions. For a purely rotational flow she derived a stability criterion $\Delta t < 4/|\zeta|$, where ζ is the relative vorticity of the flow. For longer time steps, the constant acceleration scheme does not converge. Assuming a (large) relative vorticity $\zeta = 2 \times 10^{-4}\ \mathrm{s}^{-1}$, the

time step must be smaller than 6 h. Seibert (1993) also showed that even when convergence is achieved, prohibitive truncation errors can occur. If truncation errors are to be kept below 1% of the distance travelled, the time step must be shorter than 1 h for $\zeta = 2 \times 10^{-4}\ \mathrm{s}^{-1}$. Since, on the one hand in most of the situations the time step requirements will be less demanding, while on the other hand a few situations may even be more demanding, Seibert (1993) recommended to use a scheme that automatically adjusts the time step to the actual flow situation. This was already done by Maryon and Heasman (1988), who used the difference between the constant and the variable acceleration scheme to estimate the truncation error. If the smallest features resolved by the wind data are to be reproduced in the trajectories, no grid cell must be skipped during a time step. Thus, the Courant–Friedrichs–Lewy criterion $\Delta t < \Delta x_i / |v_i|$, where Δx_i are the grid distances and v_i are the wind components, may serve as an upper limit for the flexible time step (Seibert, 1993).

2.4.2. Interpolation errors

Wind data are available only at discrete locations in space and time, either as irregularly spaced observations or as the gridded output of meteorological models. In either case, the wind speed must be estimated at the trajectory position by the trajectory model. This *interpolation* causes errors that affect the trajectory accuracy substantially.

Most trajectory models are based on gridded wind fields, but since radiosondes are the most important data for analyzing wind fields, it is interesting to discuss the errors caused by interpolation of radiosonde winds. Kahl and Samson (1986) selected three reference sites in the United States and tried several interpolation methods to estimate the wind vectors at these sites from all other radiosonde measurements. They found mean spatial interpolation errors in the horizontal wind components at an altitude of 1000 m of 3–4 $\mathrm{m\,s}^{-1}$. The temporal interpolation errors were of similar magnitude. Kahl and Samson (1986) developed what they called a "trajectory of errors" procedure. They calculated an *error trajectory*, assuming that at each time step a normally distributed error with a standard deviation determined from the interpolation experiments occurs. Conducting a Monte Carlo simulation, Kahl and Samson (1986) found a mean trajectory position error after 72 h travel time of 400 km. However, since their approach did not account for the growth of trajectory errors in divergent wind fields, this might be an underestimation. In a different estimation, Kahl and Samson (1988a) found a lower limit of the mean trajectory error caused by interpolation of 100 km after 24 h travel time for the same data set. Kahl and Samson (1988b) repeated their study for another dataset gathered during highly convective conditions and found larger average interpolation errors of 5 $\mathrm{m\,s}^{-1}$, yielding estimated mean trajectory position errors of 500 km after 72 h.

To examine the errors caused by interpolation from wind fields produced by prognostic meteorological models (either forecasts or initialized analyses), the usual method is to artificially degrade the grid resolution, interpolate the wind data to the original grid and compare with the undegraded data. Also, the temporal resolution may be varied. Stohl et al. (1995) evaluated the performance of several different interpolation methods. They found that linear interpolation is most accurate *in time*, but interpolation methods of higher order reduce errors *in space* as compared to linear interpolation. Similar results for spatial interpolation were obtained by Walmsley and Mailhot (1983). Stohl et al. (1995) also found that interpolation of the vertical wind component w produces larger errors than the interpolation of the horizontal components because of its high-frequency variability.

The effect of degrading the wind field resolution on trajectory accuracy was addressed in several studies (Kuo et al., 1985; Doty and Perkey, 1993; Rolph and Draxler, 1990; Stohl et al., 1995). One finding of these studies is that the growth of trajectory position errors with travel time caused by interpolation is approximately linear, but the most important result is that the spatial and temporal resolution of the wind fields must be in balance in order to limit the trajectory errors. An increase in spatial resolution alone does result in just marginally more accurate trajectories when the temporal resolution is low. On the contrary, increasing the temporal resolution alone is also not very effective when the spatial resolution is low. In any case, a minimum resolution of 6 h is necessary if any diurnal variations in the flow field are to be resolved.

As an example, the results of Rolph and Draxler (1990) are summarized in Table 1. At high spatial resolution, trajectories are more sensitive to a reduction of the temporal resolution than to a reduction of the horizontal resolution. However, at 360 km resolution, except for the 12 h case, the coarse spatial resolution becomes the dominant reason for trajectory errors.

The effect of interpolation errors on trajectory accuracy may also depend on the complexity of the flow situation. Stohl et al. (1995) found larger sensitivity to interpolation errors for trajectories crossing the Alps than for others. On the contrary, the sensitivity to interpolation errors did not depend on the starting

Table 1. Mean horizontal trajectory position deviations (km) from the high-resolution reference trajectories after 96 h travel time for varying spatial and temporal resolutions of the input data as found by Rolph and Draxler (1990)

Spatial resolution (km)	Temporal resolution			
	2 h	4 h	6 h	12 h
90	0	250	411	734
180	166	281	418	733
360	417	444	517	730

position of the trajectories (either in or outside a tropopause fold) in the study of Scheele et al. (1996).

2.4.3. Errors resulting from certain assumptions regarding the vertical wind

Trajectory errors are also related to different assumptions regarding the vertical wind component w. In contrast to the horizontal wind, there are no routine observations of w. Fields of w are a sole product of meteorological models, and hence they are less accurate than the fields of the horizontal wind. Sardeshmukh and Liebmann (1993) compared circulation analyses of the European Centre for Medium-Range Weather Forecasts (ECMWF) and the U.S. National Meteorological Center (NMC) for the tropics. They found a signal to noise ratio of the divergence of the horizontal wind at 200 hPa of only 2.1 : 1. Since w is balanced by the vertically integrated horizontal wind divergence, this shows the large uncertainty of w at low latitudes, mainly caused by difficulties in the parameterization of cumulus convection which is also of significance at higher latitudes during the summer. Nevertheless, if accurate fields of w are available, *three-dimensional* trajectories are more accurate than all the others (Martin et al., 1987, 1990; Stohl and Seibert, 1997).

Fuelberg et al. (1996) pointed out that it is important to obtain vertical velocities directly from a dynamically consistent numerical model. Vertical motions diagnosed from the horizontal wind components using the principle of continuity are much less accurate. Trajectories computed with these vertical motions sometimes experience unrealistically large diabatic heating or cooling rates, whereas dynamically consistent vertical motions keep the diabatic heating and cooling rates within the limits expected from theory.

The simplest alternative to three-dimensional trajectories is the neglection of w, resulting in *two-dimensional* trajectories in different coordinate systems. Often used are *isobaric* trajectories, but they are the least realistic; they may even travel below the topography. Also popular are terrain-following trajectories, e.g. the *isosigma* trajectories, for which $\sigma = (p - p_t)/(p_s - p_t)$ is kept constant (where p is the pressure, p_s the pressure at the ground and p_t the pressure at the highest model level). They may be better than isobaric trajectories in mountainous areas, but they neglect vertical motions of synoptic origin.

In *isentropic* coordinates, trajectories are truly two-dimensional under adiabatic and inviscid conditions (Danielsen, 1961; Petersen and Uccellini, 1979; Merrill et al., 1985, 1986; Artz et al., 1985). However, large problems are encountered in the PBL and in saturated moist air, where diabatic effects are most important. Draxler (1996a) demonstrated that isentropic and three-dimensional trajectories resemble each other closely during most of the time (90%), but can differ substantially when they enter baroclinic regions of the troposphere. Stohl and Seibert (1997) found that isentropic trajectories are affected more than oth-

ers by *dynamical inconsistencies* between subsequent wind fields which occur when a sequence of wind *analyses* is used for the trajectory calculations.

In the PBL, the concept of a trajectory being representative for the path of an air parcel does not hold; such a parcel quickly looses its identity by turbulent mixing. Stochastic Lagrangian particle dispersion models (see Section 4.1) can be applied to simulate the transport in the PBL, but they are demanding on computer resources and not generally applicable. Several simple methods have been proposed instead to approximate transport processes in the PBL by single trajectories. Often used are trajectories that are advected with the *vertically averaged wind* in the PBL (Heffter, 1980; Rao et al., 1983). This approach was found to agree best with the dispersion of tracer material (Haagenson et al., 1987, 1990). Harris and Kahl (1994) combined it with the isentropic concept, switching between layer-averaged advection close to the ground and advection on isentropic surfaces above.

If the PBL height fluctuates, transport of tracer material is even more complex. It may be advected partly in the PBL and partly in nighttime *residual layers* aloft. One approach (Henmi, 1980; Heffter, 1983; Comrie, 1994) is to branch a trajectory between boundary and free tropospheric layer at each transition between day and night. Another approach is to average the wind not within the boundary layer, but up to the top of the pollutant reservoir layer (Stohl and Wotawa, 1995). However, all these methods give only crude approximations of the real complexities encountered in turbulent flow.

2.4.4. Wind field errors

In many cases, errors of the underlying wind fields are the largest single source of error for trajectory calculations. Wind field errors can be due to either *analysis errors* or *forecast errors*, depending on the type of wind fields used. Trajectory errors caused by erroneous forecasts are relatively simple to evaluate by comparing forecast with analysis trajectories. Maryon and Heasman (1988) studied a one-year collection of 950 hPa forward trajectories computed from wind fields generated by a NWP model. For trajectories released at $T = 0$ (at the begin of the forecast), the mean position error after 36 h travel time was 245 km, whereas for trajectories released at $T = +36$ h (36 h into the forecast period) the mean position error after 36 h was 720 km or 60% of the distance travelled.

Stunder (1996) compared a one-year set of forecast and analyzed three-dimensional 48 h trajectories starting at altitudes of 500, 1000 and 1500 m at $T = 0$ h. She found approximately linear separation rates of 200 km/day. After 12 h, the mean position error was between 30 and 40% of the distance travelled. Trajectories with minimum relative errors tended to originate within strong steady flow either ahead or behind a cold front. Trajectories with maxi-

mum relative errors originated within high pressure systems. Haagenson et al. (1990) found forecast trajectory errors of 400 km d^{-1} for a set of 20 boundary layer trajectories that were started at $T = +5$ h. They reported smaller separation rates of 200 km d^{-1} for analysis trajectories. Stohl (1996a) investigated a one year set of terrain-following 96 h *back* trajectories at a level of 800 m above ground terminating at $T = +24$, $T = +48$ and $T = +72$ h. He found relative errors at the origin of the trajectories of 16, 26 and 36% of the travel distance, respectively. Investigations of forecast trajectories also have been presented by Heffter et al. (1990) and Heffter and Stunder (1993). Summarizing the above findings, it must be concluded that forecast errors can have a large effect on trajectory accuracy. Even for calculations that extend only shortly into the forecast period, average position errors of 30% are typical. One possibility to assess the uncertainty of forecast trajectories on-line would be to use ensemble prediction products, provided for instance by the ECMWF.

The evaluation of trajectory errors caused by wind field *analysis* errors can be done by comparing trajectories calculated from different analysis data sets. Kahl et al. (1989a, b) applied an isobaric model to 850 and 700 hPa analyses provided by the ECMWF and the NMC. The median separation between the trajectories after 120 h was 1000 km. Pickering et al. (1994) made a similar comparison of isentropic trajectories based on wind analyses of the ECMWF and the NMC. Their area of study was the South Atlantic, a region with scarce observational data. The average separation of the trajectories was approximately 1500 km after 120 h travel time and nearly 2500 km after 192 h travel time, approximately 60% of the distances travelled! Pickering et al. (1996) argued that the ECMWF analyses may be slightly more accurate than the NMC analyses in that data scarce region. Isentropic trajectory separations were slightly smaller in this more recent study, probably caused by an improvement in the NMC analysis scheme. However, they also showed that three-dimensional trajectories are even more affected by analysis errors than isentropic trajectories.

2.4.5. Starting position errors, amplification of errors, and ensemble methods

The starting positions of the trajectories are often not exactly known. For example, estimations of the effective source height of accidentally released material are usually very inaccurate. Another uncertainty is due to the differences between the model topography and the real topography, making the selection of a starting height difficult. Although the initial trajectory position error may be rather small, it can strongly amplify in *divergent* (forward trajectories) or *convergent* (back trajectories) flow.

To account for such effects, Merrill et al. (1985) started an *ensemble* of trajectories with slightly differing initial positions. In most cases, the ensembles

stayed close together, but in a few cases the trajectory end points covered a very large region, indicating large uncertainty. The use of ensemble methods was also encouraged by Seibert (1993) and their capacity for assessing trajectory uncertainty was demonstrated by Baumann and Stohl (1997) in a comparison with balloon tracks. Although the ensemble method does not produce more accurate trajectories, it gives a reliable estimation of the sensitivity of the trajectories to initial errors and other errors.

Kahl (1996) used a set of stochastic trajectories with random wind components typical for interpolation errors added at each time step to the mean wind to determine a "*meteorological complexity factor*" (MCF), defined as the average separation distance between the stochastic trajectories and a reference trajectory. He assumed that trajectory uncertainty can be predicted as a function of the MCF but since the magnitude of the MCF depends critically on the integration time step, this method might not be generally applicable.

An ensemble should ideally consist of trajectories started within a four-dimensional domain, scaled by the horizontal, vertical and temporal resolution of the wind fields and with random interpolation errors added at each time step. There remains, however, the difficulty to find the most appropriate scaling factors for the initial position displacements and for the interpolation errors. The random interpolation errors should be autocorrelated, since otherwise their effect would depend on the integration time step. Unfortunately, it is virtually unexplored how to design an ensemble method such that it gives a quantitative estimation of the trajectory uncertainty.

3. Accuracy of trajectories: tracer studies

The overall accuracy of a trajectory is determined by the integral effect of all errors discussed in the previous section. Its assessment is difficult because it requires the determination of a "*true*" reference trajectory. Except for laboratory studies (Tajima et al., 1997), this is only possible by tagging an air parcel by a *tracer* that is conserved along the trajectory. Many different tracers have been used, but none of them is ideally suited, either because it is not conserved well enough, because its determination is difficult, or because it is not normally available. Studies based on three different classes of tracers, namely balloons, material and dynamical tracers, can be found in the literature. Table 2 summarizes some of the results.

3.1. Balloons

Different types of balloons can be used for trajectory evaluations, but most studies have been done with *constant level balloons* which are intended to remain on constant density surfaces (Angell and Pack, 1960; Angell et al., 1972;

Table 2. Absolute and relative trajectory errors reported in the literature

Type of errors	Evaluated against	Comment	Travel time (h)	Errors	Reference
Truncation	Traj. computed with short integration time steps	Errors resulting from time step of 3 h using zero (constant) [variable] acceleration method	42	300 (100) [40] km	Walmsley and Mailhaut (1983)
Interpolation	Zero-interpolation error traj.	Superposition of stochastic interpolation errors occurring along traj.	72	400 km	Kahl and Samson (1986)
Interpolation	Zero-interpolation error traj.	Same as above, but for more convective conditions	72	500 km	Kahl and Samson (1988b)
Temporal interpolation	Calculated traj.	3-month set of 3-D traj. calculated from wind fields of 12 h (6 h) [4 h] time resolution vs. 2 h time resolution	96	730 km (410 km) [250 km]	Rolph and Draxler (1990)
Temporal interpolation	Calculated traj.	86 3-D traj. in an intense cyclone calculated from wind fields of 6 h (3 h) [1 h] time resolution vs 15 minutes time resolution	36	250 km (170 km) [30 km]	Doty and Perkey (1993)
Temporal interpolation	Calculated traj.	1-yr set of 3-D (2-D) traj. calculated from wind fields of 6 h time resolution vs 3 h time resolution	96	590 km, 20% (280 km, 9%)	Stohl et al. (1995)
Horizontal interpolation	Calculated traj.	3-month set of traj. calculated from wind fields of 360 km (180 km) resolution vs 90 km resolution	96	420 km (170 km)	Rolph and Draxler (1990)
Horizontal interpolation	Calculated traj.	1-yr set of 3-D (2-D) traj. calculated from wind fields of 1° resolution vs 0.5° resolution	96	411 km, 14% (111 km, 4%)	Stohl et al. (1995)
Forecast	Analysis traj.	1-yr set of 950 hPa forward traj. started at $T = 0$ h ($T = +36$ h)	36	245 km, 25% (720 km, 60%)	Maryon and Heasman (1988)
Forecast	Analysis traj.	1-yr set of forward 3-D traj. started 500, 1000, 1500 m above ground	> 12	200 km/day	Stunder (1996)

Table 2. (Continued)

Type of errors	Evaluated against	Comment	Travel time (h)	Errors	Reference
Forecast	Analysis traj.	1-yr set of back traj. travelling 800 m above ground terminating at $T = +24$ h ($T = +48$ h) [$T = +72$ h]	96	16% (26%) [36%]	Stohl (1996a)
Wind field analysis	ECMWF traj. compared to NMC traj.	Isobaric 850 and 700 hPa traj.	120	1000 km	Kahl et al. (1989a, b)
Wind field analysis	ECMWF traj. compared to NMC traj.	Isentropic traj. over the south Atlantic	120 (192)	1500 km, 60% (2500 km, 60%)	Pickering et al. (1994)
Total	Constant level balloon	26 cases, diagnostic wind field model used	< 24	25–30%	Clarke et al. (1983)
Total	Constant level balloon	16 cases in and immediately above the PBL	1–3	5–40%	Koffi et al. (1997a, b)
Total	Constant level balloon	Stratospheric traj.	12–144	≈ 20%	Knudsen and Carver (1994) Knudsen et al. (1996)
Total	Manned balloon	Single flight at a typical height of 500 hPa	100	10%	Draxler (1996b)
Total	Manned balloon	4 flights at a typical height of 2000 m	46	< 20%	Baumann and Stohl (1997)
Total	Tracer (CAPTEX)	6 cases, different types of traj.	24	≈ 200 km	Haagenson et al. (1987)
Total	Tracer (CAPTEX)	6 cases	24–42	150–180 km	Draxler (1987)
Total	Tracer (ANATEX)	30 cases	< 30	20–30%	Draxler (1991)
Total	Tracer (ANATEX)	23 boundary layer traj.	24–72	≈ 100 km/d^{-1}	Haagenson et al. (1990)
Total	Smoke plumes	112 traj. based on a fine-scale (global) analysis	< 60	10% (14%)	McQueen and Draxler (1994)
Total	Saharan dust	Single case, 3-D traj.	3000 km	200 km, 7%, vertical error 50 hPa	Reiff et al. (1986)
Total	Potential vorticity	1-yr set of 3-D traj. based on ECMWF data	120	< 20%, < 400 km, vertical error < 1300 m	Stohl and Seibert (1997)

Note. The table summarizes not only total errors, but also errors caused by single error sources, such as interpolation. Different errors reported by the same author are put in parantheses.

Hoecker, 1977; Pack et al., 1978; Kahl et al., 1991). Reisinger and Mueller (1983) compared 45 tetroon flights (altitudes 300–1500 m, mean travel distance 90 km) with trajectories calculated from interpolated radiosonde measurements. They found that computed trajectories underestimated the meandering of the tetroons due to the smoothing effect of interpolation. The mean direction difference between computed and tetroon trajectories was 28°. Warner et al. (1983) highlighted the importance of prognostic models for providing high-resolution input to trajectory models, because trajectories calculated from wind analyses were smoother than tetroon trajectories. In an evaluation of several different trajectory models using 26 tetroon flights, Clarke et al. (1983) found mean errors of approximately 25–30% of the travel distance. Koffi et al. (1997a, b) found relative errors of approximately 5–40% of the travel distance for constant level balloon flights undertaken during the ETEX tracer experiment.

Knudsen and Carver (1994) and Knudsen et al. (1996) looked at stratospheric long-duration (0.5–6 d) constant level balloon flights. They found typical differences of 20% of the travel distance between trajectories calculated from ECMWF analyses and balloon trajectories. Under special circumstances, 24 and 48 h trajectories had errors exceeding 40%.

The tracks of *manned balloons* may also be used for comparison with calculated trajectories, if changes in the balloon heights are accounted for (Wetzel et al., 1995). Draxler (1996b) found an error of 10% of the travel distance for a 100 h transpacific balloon flight at a level of approximately 500 hPa. Baumann and Stohl (1997) evaluated trajectories calculated from ECMWF analyses using four gas balloon flights (typical height 2000 m) of 46 to 92 h duration and found errors of 4–45% of the distance travelled. The average error after 46 h was less than 20%.

Stocker et al. (1990) used 190 000 tagged helium-filled latex balloons launched from 800 sites around the United States of which 4.5% were later found and returned. Balloon and calculated boundary layer trajectory motion were often in complete disagreement, especially under light wind conditions. Similar difficulties were reported by Baumann et al. (1996) based on a study of hot-air balloon flights in complex terrain.

The obvious disadvantage of all balloon-based studies is that balloons do *not* follow the real three-dimensional air motions, but tend to stay on pressure surfaces or actively change height (manned balloons). Therefore, errors in the vertical wind are not detected.

3.2. Material tracers

There are two groups of material tracers, *material tracers of opportunity*, such as smoke plumes or geochemical tracers, and *inert tracer gases* released dur-

ing specifically designed experiments. Tracers of opportunity may be available without the high costs and efforts of planned tracer experiments, but usually the source position, strength and/or release time of the tracer material are not accurately known. This problem is not encountered within tracer experiments, but only a few well-documented data sets on the regional to continental scale are available.

3.2.1. Tracer experiments

Different chemical compounds have been used as tracers, basic requirements being that the material must be chemically stable, not subjected to wash-out, rain-out or dry deposition, non-toxic, environmentally safe, detectable at low concentrations, and must have near-zero background concentrations. Sulfur hexafluoride (SF_6) on the local scale (Lamb et al., 1978a, b) and perfluorocarbons on the regional to continental scale (Draxler, 1991) have often been used. We will focus on regional to continental scale tracer experiments, because short-range experiments are usually conducted to study turbulent flows for which the accuracy of single trajectories can hardly be judged.

Three tracer experiments received the most interest until now. The first one was the *Cross-Appalachian Tracer Experiment* (CAPTEX), conducted during September and October 1983 (Ferber et al., 1986). A total of seven releases of a perfluorocarbon was made when winds were predicted to carry it over the ground-level sampling network (80 sites) which covered the northeast United States and Canada.

Haagenson et al. (1987) analyzed the tracer data to a grid and derived *tracer trajectories* that tracked the location of the tracer plume centroid. They pointed out that this definition of the tracer trajectories is somewhat arbitrary, and alternative definitions might be used as well. With the tracer trajectories, they evaluated several types of trajectories and came to the conclusions that surface winds should not be used to simulate PBL transport, that wind flow corresponding to the low to middle PBL is much more appropriate, that isentropic, layer-averaged and isosigma trajectories are more realistic than isobaric trajectories, and that average errors after 24 h travel time were approximately 200 km.

Draxler (1987), using the same dataset, found smaller trajectory errors (150–180 km as the average for 24–42 h travel time); isentropic trajectories were more accurate than isosigma trajectories; increasing the spatial *and* temporal resolution of the wind fields (using additional radiosondes) improved the trajectory accuracy significantly, whereas increasing spatial or temporal resolution alone did not improve it. Chock and Kuo (1990) compared trajectories computed from model predicted wind fields with trajectories computed from objective wind analyses. They stated that the former were more accurate, especially in the presence of fronts, but gave no quantitative measure of accuracy.

Determining a tracer trajectory from the surface concentration pattern is difficult, because the spatial structure of the tracer concentrations depends also on other factors than the horizontal transport. Shi et al. (1990) used a Lagrangian particle model to simulate three CAPTEX releases. Since the calculated tracer plumes at higher levels looked very different from the calculated ground-level plumes, they concluded that comparisons with the surface tracer concentration footprint are not ideally suited to assess the accuracy of trajectories, because differences in vertical mixing can lead to substantially different horizontal trajectories due to the vertical shear of the horizontal wind.

The *Across North America Tracer Experiment* (ANATEX) was conducted from January to March 1987 (Draxler et al., 1991). 33 releases of different tracer gases were made simultaneously from each of two locations every 2.5 days, alternating between daytime and nighttime releases. Ground-level air samples of 24 h duration were taken at 77 sites situated throughout North America and air samples of 6 h duration were taken at 5 towers.

Haagenson et al. (1990) used tracer-derived trajectories to validate calculated trajectories. Layer-averaged trajectories performed best (separation rate 180 km d^{-1}), but isosigma trajectories were nearly equally good. The rate of increase of the trajectory error decreased slightly with time. Although three-dimensional trajectories were generally similar to isosigma trajectories, large upward displacement of the trajectories was associated with low tracer concentrations at the surface. Dispersion models based on two-dimensional trajectories may thus overpredict surface tracer concentrations. Haagenson et al. (1990) also used different types of meteorological data (objective analyses, forecasts, four-dimensional data assimilation) to drive the trajectory model. They found that the quality of the forecasts (96 h forecasts initiated 5 h prior to the tracer release) was much lower than the quality of the analyses. This is in direct contradiction to Chock and Kuo's (1990) study based on the CAPTEX data. Possible reasons for this are the longer forecast period used for the ANATEX data and the more complex meteorological conditions.

Draxler (1991) used aircraft measurements available for 30 ANATEX releases and calculated *back trajectories* from the tracer centroid positions to minimize the complications introduced in comparing trajectories while also having to model the vertical diffusion. He defined the trajectory error to be the nearest distance of a trajectory to the tracer origin point. He compared short-term forecasts of the Nested Grid Model (NGM) that were initialized every 12 h with analyses of radiosonde observations. Both for the NGM forecasts and for the analyses, transport errors were approximately 20–30% of the distance travelled.

The most recent tracer experiment on a continental scale was the *European Tracer Experiment* (ETEX) in October to November 1994 with two releases of a perfluorocarbon tracer from a site in western France. The sampling network

provided high spatial (168 stations) and temporal (3 h) resolution (Mosca et al., 1997). The major task of ETEX was to evaluate real time forecasting of the tracer concentration field (Archer et al., 1996) as well as subsequent model analyses of the transport patterns, but the data set could be also used to explore the accuracy of trajectories.

3.2.2. Tracers of opportunity

Any detectable material that is conserved along trajectories may serve as a tracer; for instance pollen (Raynor et al., 1983), volcanic ash (Heffter et al., 1990; Heffter and Stunder, 1993) or the radioactive emissions from the Chernobyl accident (Kolb et al., 1989; Klug et al., 1992). Reiff et al. (1986) studied an episode of African dust transport to northwestern Europe. They used satellite imagery, upper-air soundings, surface observations, X-ray analyses of the dust composition and low-level dust-concentration measurements to determine the place of origin and the path of the desert dust. Independently calculated trajectories based upon wind analyses produced at the ECMWF tracked the dust cloud very accurately (error less than 200 km after a travel distance of 3000 km). Also the vertical displacements calculated by the model could be confirmed by the measurements (error less than 50 hPa). Martin et al. (1990) investigated several episodes of Saharan dust transport to the Mediterranean. They also suggested that the vertical wind component should be used for the trajectory computations.

McQueen and Draxler (1994) used the smoke plumes from the Kuwait oil fires during the Gulf war to evaluate the accuracy of trajectories. They determined the plume centerline from satellite data and the vertical plume position by comparing back trajectories released at different heights. They assumed that the plume centroid height is identical to that of the trajectory that most accurately tracked the plume back to the burning oil fields. Using a global analysis and a fine-scale analysis, they found trajectory errors of 10% for the fine grid and 14% for the coarse grid. Since the plume height was determined by the "best" trajectory, this is likely to be an underestimation of the "true" error.

3.3. Dynamical tracers

One dynamical tracer is *potential temperature* which is often used to constrain the vertical motion of trajectories (isentropic assumption). Another tracer is *isentropic potential vorticity* (PV) that is conserved for inviscid adiabatic motions (Davis, 1996). It is defined by

$$\mathrm{PV} = -g\eta_\Theta \frac{\partial \Theta}{\partial p} \tag{13}$$

with $\eta_\Theta = \zeta_\Theta + f$, ζ_Θ being the relative vorticity on an isentropic surface, and g the gravitational acceleration. PV has been used sometimes to study the accuracy of individual trajectories (Artz et al., 1985; Jäger, 1992). However, Knudsen and Carver (1994) found that due to the high-frequency variability of PV, difficulties in its analysis and its non-conservation under diabatic conditions, only large PV changes can be taken as an indication of individual trajectories being wrong.

Nevertheless, PV is very useful in a statistical framework. Recently, Stohl and Seibert (1997) studied PV conservation to determine the average accuracy of a large set of trajectories calculated from ECMWF analyses. They found that three-dimensional trajectories were the most accurate trajectory type, followed by kinematic isentropic trajectories. Isobaric trajectories were clearly less accurate. Average relative horizontal position errors for three-dimensional trajectories were estimated to be less than 20% for travel times longer than 24 h in the free troposphere. Tentative upper bounds for average absolute horizontal and vertical errors after 120 h travel time were 400 km and 1300 m, respectively.

4. Applications of trajectories

4.1. Lagrangian particle dispersion models

Although trajectory models have been used successfully to study complex transport processes such as recirculation of pollutants (Tyson et al., 1996), it is virtually impossible to describe transport phenomena in *turbulent flows* by calculating single trajectories. More sophisticated models are needed, both in the PBL, where an air parcel quickly looses its identity due to strong mixing (Lyons et al., 1995), and at higher levels of the atmosphere when longer time scales are considered (Sutton, 1994). These models can be either Eulerian transport models or Lagrangian particle dispersion models (LPDM). LPDM have no artificial numerical diffusion like Eulerian models (Nguyen et al., 1997) and hence have a greater potential to resolve fine-scale structures of the flow.

LPDM numerically simulate the transport and diffusion of a passive scalar tracer by calculating the Lagrangian trajectories of tens or hundreds of thousands of tagged "*particles*." These trajectories are calculated according to

$$\mathbf{X}(t + \Delta t) = \mathbf{X}(t) + \Delta t\left[\bar{\mathbf{v}}(t) + \mathbf{v}'(t)\right] \tag{14}$$

where $\bar{\mathbf{v}}$ is the *resolvable scale wind vector* obtained directly from a meteorological model, and $\mathbf{v}'$ is the *turbulent wind vector* that describes the turbulent

diffusion of the tracer in the PBL. The concentration of the tracer at a specific location at a given time is linearly proportional to the number of particles per unit volume. It can be evaluated simply by counting all particles that reside within a certain volume or, more favorably, by using a kernel method (Lorimer, 1986; Uliasz, 1994).

Different alternative names are given to LPDM; e.g. Langevin, Markov chain, Monte Carlo, random walk, and stochastic Lagrangian (Rodean, 1996), each referring to a certain attribute of the models. See Thomson (1984, 1987), Wilson and Sawford (1996) and Rodean (1996) for detailed treatments of the mathematical and physical background of LPDM, and Uliasz (1994) and Zannetti (1992) for discussions of more practical aspects of LPDM simulations.

The core problem of LPDM is the determination of the turbulent velocities $\mathbf{v}'$. Turbulent diffusion, like molecular diffusion (*Brownian motion*), can be described as a *Markov process*, a stochastic process that has a future that depends only on its present state and a transition rule. The particles forget their current velocity state after some time characterized by the *Lagrangian time scale*. This is written as the *Langevin equation* (Thomson, 1987)

$$\mathrm{d}v_i' = a_i(\mathbf{X}, \mathbf{v}', t)\mathrm{d}t + b_{ij}(\mathbf{X}, \mathbf{v}', t)\mathrm{d}W_j(t) \tag{15}$$

where a and b are functions of $\mathbf{X}$, $\mathbf{v}'$ and t and the $\mathrm{d}W_j$ are the increments of a vector-valued *Wiener process* with independent components. The $\mathrm{d}W_j$ represent Gaussian white noise with mean zero and variance $\mathrm{d}t$; increments $\mathrm{d}W_i$ and $\mathrm{d}W_j$ occurring at different times, or at the same time with $i \neq j$, are independent.

For instance, given a state n of the turbulent vertical velocity w' of a particle at time t, a future state $n+1$ at time $t + \Delta t$ can be determined using the autocorrelation coefficient $r = \exp(-\Delta t/\tau_{\mathrm{L}})$ with τ_{L} being the Lagrangian time scale for w' (Wilson et al., 1983)

$$\frac{w'^{n+1}}{\sigma_w^{n+1}} = r\,\frac{w'^{n}}{\sigma_w^{n}} + \chi\sqrt{(1-r^2)} + (1-r)\tau_{\mathrm{L}}\,\frac{\mathrm{d}\sigma_w}{\mathrm{d}z} \tag{16}$$

where χ is a normally distributed random number and σ_w is the root-mean-square Eulerian turbulent vertical velocity. Both τ_{L} and σ_w can be calculated diagnostically based on certain boundary layer characteristics (Hanna, 1982) or can be related to the turbulent kinetic energy (Fay et al., 1995). Using sufficiently small time steps, Eq. (16) fulfills the most important criterion for an LPDM, the "*well-mixed*" criterion, which states that if the particles of a passive tracer are initially mixed uniformly in a turbulent flow, they will remain so (Thomson, 1987). Only models that fulfill this criterion are physically correct.

The last term on the right-hand side of Eq. (16) is the *drift correction velocity*, introduced by Legg and Raupach (1982) in a similar, albeit, as was found later, not correct form in order to avoid the accumulation of particles in regions of low turbulence which would violate the well-mixed criterion (McNider et al., 1988). Special attention must be paid to flow boundaries (i.e. the ground and the top of the PBL), where particles are reflected (Wilson and Flesch, 1993; Thomson and Montgomery, 1994).

Usually, Gaussian turbulence is assumed in an LPDM, but under convective conditions vertical tracer transport occurs primarily in *updrafts* and *downdrafts*. Updrafts have higher velocities but occupy less area than downdrafts leading to a skewed vertical velocity distribution (Luhar et al., 1996). Baerentsen and Berkowicz (1984) approximated this by the sum of two Gaussian distributions, one for the updrafts and the other for the downdrafts.

There exist several approaches to deal with the turbulent horizontal velocities. The simplest solution is to solve an independent Langevin equation for all three wind components, but measurements of wind fluctuations indicated that there exist cross-correlation terms between the individual wind components (Zannetti, 1992). These cross-correlations can be very important near the source, but Uliasz (1994), who compared an LPDM simulation that accounted for the cross-correlations with another that did not, found that in mesoscale applications the cross-correlations are not important. Actually, the horizontal turbulent velocities had little effect at all, even when they were completely neglected.

Another simplification to save computing time is to neglect the autocorrelations of the turbulent wind components or to increase the model time step above the Lagrangian timescale. This is equivalent to converting the Markov process for the velocity *and* position of the particles into one for their position only. Uliasz (1994) showed that even this gross simplification had no large effects on the simulated tracer concentrations in regional applications. The reason for this is that the most important process affecting the regional-scale tracer dispersion is the evolution of the PBL height along the particles path and the formation of tracer reservoir layers above the PBL. The details of the transport within the PBL are not so important since the temporal scale of vertical mixing is much shorter than the transport times. However, Maryon and Buckland (1994) argued that errors near the source caused by an oversimplified dispersion algorithm could translate into much larger errors at later times. A compromise to save computation time while maintaining sufficient accuracy would therefore be to use short time steps close to the source, but longer ones when the tracer is already well-mixed within the PBL.

Validations of LPDM are usually based on tracer experiments (Shi et al., 1990; Eastman et al., 1995; Fay et al., 1995; Moran and Pielke, 1996) or on tracers of opportunity (Draxler et al., 1994; Uliasz et al., 1997). The best way

to validate LPDM is to compare modeled concentrations at the locations of the measurement sites to the measured concentrations. This method does not require to interpolate the measurements to a regular grid, which introduces substantial uncertainties. This validation strategy was followed systematically in the model evaluation study following the ETEX experiment (Mosca et al., 1997). The major remaining difficulty is the definition of the statistical measures most suitable for model evaluation.

LPDM can simulate, in addition to the dispersion, all linear processes, such as dry and wet deposition, radioactive decay, and linear chemical transformations, but a major drawback is that, currently, non-linear chemical reactions cannot be accounted for. There exist experiments to compute the chemical transformations on a grid based on the concentrations predicted by the LPDM (Chock and Winkler, 1994a, b) and to subsequently re-transform the gridded concentrations to particle masses, but these models are not yet operational, an exception being the study of Stevenson et al. (1997).

Traditionally, LPDM are used to obtain a time- and space-varying concentration field for a given emission scenario. However, because all processes simulated by an LPDM are linear, the inverse modeling is simple. Computing back trajectories from a given receptor location, a time- and space-varying *influence function* can be obtained (Uliasz, 1994). It is independent of a certain emission scenario and can therefore be used to calculate the pollutant concentration at the receptor for multiple emission scenarios without having to re-run the model. Since this receptor-oriented approach is computationally efficient, it is also possible to compute long-term concentration time series (Uliasz et al., 1997). It would be rewarding to examine these influence functions for long-term simulations using methods similar to the trajectory statistics presented in Section 4.3 to construct emission fields. A different method to estimate emissions from concentration measurements combined with backward LPDM simulations was presented by Flesch et al. (1995) and Flesch (1996), but this approach requires that the geometry of the source is known beforehand.

Finally, some attention shall be drawn to a problem of current LPDM that—to the author's knowledge—has not yet been solved: all procedures available to calculate $\mathbf{v}'$ assume constant density flows. This might be a justified approximation for shallow stable PBLs but certainly not for deep convective PBLs. There, density differences of 20% between the bottom and the top are typical. Neglect of these differences—as it is current practice—leads to an underestimation of ground-level concentrations and an overestimation of concentrations at the PBL top, which also translate into transport errors. Therefore, it would be a rewarding task to derive a Langevin equation that accounts for density fluctuations.

4.2. Lagrangian box models

LPDM have not yet been combined with nonlinear chemical reaction schemes because of the conceptual difficulties mentioned above, but Lagrangian *box models* have been very popular because of their computational efficiency. If the concentrations of some chemical species at a specific location are to be modeled, first a *back* trajectory is calculated from this location. Then, a box is moved *forward* along this trajectory and changes in the concentrations in the box caused by chemical reactions and deposition are calculated. Compared to *zero-dimensional* Eulerian models, Lagrangian box models are more practical because no advection from outside the box occurs and hence no *boundary conditions* are required. However, such models are fully applicable only at higher levels of the atmosphere (Sparling et al., 1995) where turbulence is weak. For models used in the PBL (Eliassen et al., 1982), the height of the box must be adjusted to the variations of the PBL height, allowing air to be entrained from above which requires the specification of boundary conditions.

Lagrangian column models calculate the exchange of air between boxes arranged in a column. The most important boundary layer processes, such as the formation of nighttime reservoir layers or the rapid growth of the mixed layer depth in the morning, can be described with such models (Hertel et al., 1995), while their computational requirements are still moderate. For the calculation of the turbulent vertical exchange it is necessary that the boxes of the column remain exactly above each other. In reality, however, a vertical shear of the horizontal wind would separate the boxes. To avoid this *grid tangling*, the wind shear must be neglected and the whole column of boxes must be advected along a single trajectory. It is for this reason Lagrangian column models are less accurate than three-dimensional Eulerian models (Peters et al., 1995). Therefore, Lagrangian models are used mainly when computational costs are too high for Eulerian models, such as for long-term studies (e.g. De Leeuw et al., 1990) or when very complex chemical reaction schemes are applied (e.g. Derwent, 1990). They might be useful also for assimilating observations to produce accurate analysis maps of chemical species (Fisher and Lary, 1995), an application that is still extremely costly using Eulerian models.

4.3. Statistical analyses of trajectories

Trajectories have been used to interpret individual flow situations for several decades now, but statistical analysis methods for large sets of trajectories have been developed more recently. An early bibliography of such methods was prepared by Miller (1987), but more sophisticated methods have evolved since then.

4.3.1. Flow climatologies

The first statistical trajectory analyses were *flow climatologies*: back trajectories were calculated over a time span of several years and their transport directions and travel speeds were classified according to some criteria. These criteria were defined to discriminate, for instance, between oceanic, clean continental and polluted continental air masses.

An early example of this technique is the study of Miller (1981). He calculated more than 7000 back trajectories and classified them into five transport sectors. Many authors used variations of this technique, mostly to group air and precipitation chemistry data to identify roughly the source areas of air pollutants, namely those transport sectors associated with high pollutant concentrations at the receptor site (Henderson et al., 1982; Colin et al., 1989; Miller et al., 1993; White et al., 1994). For a bibliography see Miller (1987).

4.3.2. Cluster analysis

Cluster analysis is a *multivariate* statistical technique that splits a data set into a number of groups. Cluster analysis is often described as an *objective* classification method, but this is not true since the selection of the clustering algorithm, the specification of the distance measure and the number of clusters used are *subjective*. Kalkstein et al. (1987), who evaluated three different clustering procedures for use in synoptic climatological classification, remarked to the problem of subjectivity: "The selection of the proper clustering procedure to use in the development of an objective synoptic methodology may have far-reaching implications on the composition of the final 'homogeneous' groupings."

Cluster analysis has only recently been applied to meteorological data (Kalkstein et al., 1987; Fernau and Samson, 1990a, b; Eder et al., 1994). Moody and Galloway (1988) were the first to consider trajectory coordinates as the clustering variables. In principle, the result of a cluster analysis is similar to a flow climatology (which means trajectories are classified into some groups), but cluster analysis is *more* objective, and it accounts for variations in transport speed and direction simultaneously, yielding clusters of trajectories which have similar length and curvature (Moody and Samson, 1989; Harris and Kahl, 1990). Harris (1992) based a flow climatology for the South Pole on cluster analysis of trajectories and Moody et al. (1995) used cluster analysis to interpret ozone concentrations. Sirois and Bottenheim (1995) applied both cluster analysis and residence time analysis (see below) to interpret a 5-yr record of PAN and O_3. Kahl et al. (1997) used cluster analysis to investigate whether clear air tends to arrive at the Grand Canyon National Park over certain

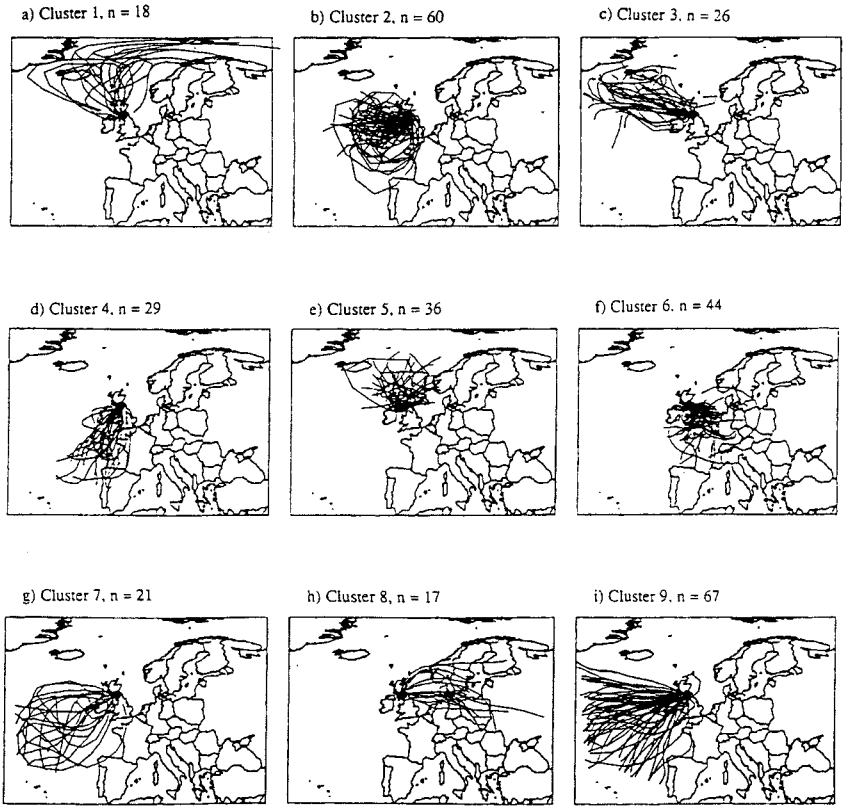

Figure 1. An example, originally presented by Dorling et al. (1992a), for the result of a trajectory cluster analysis. Shown are nine clusters identified with their trajectory members.

preferred pathways. Dorling et al. (1992b) and Dorling and Davies (1995) presented applications of trajectory clustering; the paper of Dorling et al. (1992a) contains a detailed description of their procedure which works very well in discriminating distinct flow patterns and large-scale circulation features (Stohl and Scheifinger, 1994). Fig. 1 shows as an example the result of the cluster analysis by Dorling et al. (1992a).

4.3.3. Residence time analysis and conditional probability fields

The methods discussed so far (flow climatologies, cluster analysis) classify trajectories without directly involving air pollution data. Ashbaugh (1983) and Ashbaugh et al. (1985) developed a method, *residence time analysis*, to identify source areas of air pollutants. A similar, albeit simpler, approach was pub-

lished at about the same time by Munn et al. (1984). Ashbaugh et al. (1985) calculated a large set of back trajectories, each consisting of a number of segments separated by specific time increments and characterized by their positions and time, respectively. Then they covered the area of study with a grid and defined an event A to occur if an air parcel at time t happens to be inside a certain grid cell.

If N is the total number of trajectory segments and n_{ij} is the number of points falling in the ijth grid cell during a time interval T, then the probability that a randomly selected air parcel resides in the ijth grid cell is $P[A_{ij}] = n_{ij}/N$. Next, let m_{ij} be the number of trajectory segment points in the ijth grid cell, but only for those trajectories which arrive at the receptor when a certain criterion value for the pollutant concentration is exceeded. Then, the probability $P[B_{ij}] = m_{ij}/N$ represents the residence time of high pollutant concentration air parcels in the ijth grid cell (events B_{ij}) relative to the total time period considered. First knowledge of possible source regions can be gained from the differences in the probability fields $P[B_{ij}]$ and $P[A_{ij}]$ (Poirot and Wishinski, 1986), but both probability fields have their peak values in the grid cell where the receptor site is situated because all trajectories have to pass through this grid cell. Ashbaugh et al. (1985) normalized $P[B_{ij}]$ with $P[A_{ij}]$ to eliminate the redundant information. This can be written as

$$P[B_{ij} \mid A_{ij}] = \frac{P[B_{ij}]}{P[A_{ij}]} = \frac{m_{ij}}{n_{ij}} \tag{17}$$

with $P[B_{ij} \mid A_{ij}]$ being the *conditional probability* of the event B_{ij} given that event A_{ij} occurs. Regions with high conditional probability have a large potential to adversely affect the air quality at the receptor site when they are crossed by a trajectory. They do not necessarily make a large contribution to long-term air pollutant concentrations, since this also depends on the frequency at which air parcels actually travel over that region.

Ashbaugh's method was adopted by Zeng and Hopke (1989), Hopke et al. (1993), Cheng et al. (1993a, b) and Gao et al. (1993) who used it for studies of acid precipitation, sulfate, sulfur dioxide and heavy metals. Comrie (1994) and Stohl and Kromp-Kolb (1994a) used the technique to track ozone, and Sirois and Bottenheim (1995) combined it with cluster analysis to investigate ozone and PAN concentrations. Vasconcelos et al. (1996b) investigated the spatial resolution of the method. They found that the angular resolution is good, but that the radial resolution is poor because of the convergence of all trajectories toward the receptor.

It is clear that the certainty with which the conditional probability of a grid cell is known depends on the number of events A_{ij} in that cell. Recently, Vasconcelos et al. (1996a) proposed two statistical tests to examine the signifi-

cance of conditional probability maps, one using a bootstrapping technique, the other based on a binomial distribution.

4.3.4. Concentration fields

Seibert et al. (1994a, b) computed *concentration fields* to identify source areas of air pollutants. Like Ashbaugh, they superimposed a grid to the domain of trajectory computations. Then they calculated a logarithmic mean concentration for each grid cell according to

$$\overline{C}_{ij} = \frac{1}{\sum_{l=1}^{M} \tau_{ijl}} \sum_{l=1}^{M} \log(c_l)\tau_{ijl} \tag{18}$$

where i, j are the indices of the horizontal grid, l the index of the trajectory, M the total number of trajectories, c_l the concentration observed on arrival of trajectory l and τ_{ijl} the time spent in grid cell (i, j) by trajectory l. A high value of $\overline{C}_{ij}$ means that, on average, air parcels passing over cell (i, j) result in high concentrations at the receptor site.

The fields exhibit small-scale variations which are not necessarily statistically significant. Simple smoothing of the concentration field, however, is not justified, because this would also remove many significant structures. Therefore, a confidence interval for the mean concentration of each grid cell is calculated using t-statistics based on the number of trajectories passing through each cell. Then, the concentration field is smoothed with a 9-point filter, imposing the restriction that the values must be kept within their confidence interval. The smoothing is repeated until the change in the concentration field is less than a prespecified value. This procedure assures that significant variations are preserved while most of the insignificant ones are removed. Stohl and Kromp-Kolb (1994b) used Seiberts method for an analysis of the ozone plume of Vienna.

4.3.5. Redistributed concentration fields

Sources of air pollutants are often concentrated in "hot spots", but Ashbaugh's and Seibert's procedures underestimate the spatial gradients of the "true" source fields because a measured concentration is attributed equally to all segments of its related trajectory. Let us imagine some trajectories which differ from each other, except for the fact that they all pass over one specific grid cell. Let all but one be "clean" trajectories, associated with low concentrations at the receptor site. Thus, no major pollutant source is located along their paths and specifically not in the grid cell which they share with the one "polluted"

trajectory. Therefore, the latter one must have taken up its pollutant load somewhere else. This information can be used for an iterative redistribution of the concentrations along the trajectories (Stohl, 1996b).

The major assumption of the redistribution method is that the measured species is directly emitted or produced by linear chemistry. Thus, problems are likely to occur for species produced by non-linear chemistry such as ozone. Wet deposition processes may also have a negative impact on the results. Stohl (1996b) tested the capacity of his method with particulate sulfate data measured at 14 sites in Europe and found that the concentration field was in good agreement with an emission inventory. Virkkula et al. (1995) applied the redistribution method to the concentrations of non-sea-salt sulfate, ammonium and sodium measured in the Finnish subarctic and were able to identify the very different sources of these species.

4.3.6. Inverse modeling

Recently, Seibert (1997) presented a new approach towards establishing trajectory-derived source–receptor relationships. It is not based on statistics, but on inverse modeling, viewing trajectories as the output of a primitive Lagrangian dispersion model. This is an ill-posed inversion problem, since the dimensions of the receptor-concentration-vector and of the source-vector are not equal. Seibert (1997) overcomes this difficulty by introducing additional constraints, but the effect of these constraints has to be explored further. Nevertheless, inverse modeling could be very useful in future work, especially because it can be extended more easily than trajectory statistics to the results of more sophisticated dispersion models including, for instance, wet deposition processes.

5. Summary and conclusions

In this paper, it was shown how trajectories are being calculated, how accurate they typically are and how their accuracy can be assessed. There exists some evidence (see Table 2) that the accuracy of trajectory calculations has been improved in recent years, especially since three-dimensional wind fields are available from numerical weather prediction models. There is consensus now in the literature that three-dimensional trajectories are more accurate than any other type of trajectories, including isentropic trajectories.

Nevertheless, position errors of 20% of the travel distance can still be considered as typical, limiting the general applicability of calcuated trajectories. Slightly smaller errors are often being reported for trajectories calculated from high-quality analysis fields in data-rich regions, but much larger errors, on the

order of 30% or more, are typical for forecast trajectories. Since trajectory errors vary considerably from case to case, ranging from practically zero error to trajectories heading into the opposite direction of the real trajectories, it is essential to assess the uncertainty of trajectories on an individual case basis. This can be done either by using on-line tracers, such as potential vorticity, or by using trajectory ensemble methods.

Due to turbulent mixing, single trajectories are hardly sufficient to describe transport processes in the boundary layer. LPDM provide a more adequate representation of transport in turbulent flows. Therefore, studies that are currently based on the interpretation of forward or back trajectories (for instance interpretations of the measurements of trace constituents of the atmosphere), should in the future be based on the simulation results of LPDM.

Lagrangian chemical box or column models often suffer from large errors introduced by the vertical shear of the horizontal wind that cannot be accounted for with these models. Therefore, they should only be applied when other models (Eulerian chemical transport models) cannot be used due to a lack of computer capacity. However, it would be interesting to design LPDM with nonlinear chemistry.

New methods of trajectory statistics to interpret long-term air pollutant time series have been developed in the last few years, but these methods still need considerable improvement if they shall be applied to reconstruct emission fields. A large improvement could probably be achieved if the output of LPDM could be used in the statistics instead of single trajectories.

Acknowledgements

I am grateful to Jonathan Kahl, Petra Seibert and an anonymous reviewer for their very valuable comments.

References

Angell, J.K., Pack, D.H., 1960. Analysis of some preliminary low-level constant level balloon (tetroon) flights. Monthly Weather Review 7, 235–248.

Angell, J.K., Pack, D.H., Machta, L., Dickson, C.R., Hoecker, W.H., 1972. Three-dimensional air trajectories determined from tetroon flights in the planetary boundary layer of the Los Angeles basin. Journal of Applied Meteorology 11, 451–471.

Archer, G., Girardi, F., Graziani, G., Klug, W., Mosca, S., Nodop, K., 1996. The European long range tracer experiment (ETEX). Preliminary evaluation of model intercomparison exercise. In: Gryning, S.E., Schiermeier, F.A. (Eds.), Air Pollution Modeling and its Application XI, Vol. 21. Plenum Press, New York, pp. 181–190.

Artz, R., Pielke, R.A., Galloway, J., 1985. Comparison of the ARL/ATAD constant level and the NCAR isentropic trajectory analyses for selected case studies. Atmospheric Environment 19, 47–63.

Ashbaugh, L.L., 1983. A statistical trajectory technique for determining air pollution source regions. Journal of Air Pollution Control Association 33, 1096–1098.

Ashbaugh, L.L., Malm, W.C., Sadeh, W.Z., 1985. A residence time probability analysis of sulfur concentrations at Grand Canyon National Park. Atmospheric Environment 19, 1263–1270.

Baerentsen, J.H., Berkowicz, R., 1984. Monte Carlo simulation of plume dispersion in the convective boundary layer. Atmospheric Environment 18, 701–712.

Baumann, K., Langer, M., Stohl, A., 1996. Hot-air balloon tracks used to analyze air flow in alpine valleys. Proceedings of the 24th Conference on Alpine Meteorology, Bled, Slovenia, pp. 60–66.

Baumann, K., Stohl, A., 1997. Validation of a long-range trajectory model using gas balloon tracks from the Gordon Bennett Cup 95. Journal of Applied Meteorology 36, 711–720.

Byers, H.R., 1974. General Meteorology, 4th ed., McGraw–Hill, New York, USA.

Cabezudo, B., Recio, M., Sánchez-Laulhé, J.M., Trigo, M., Toro, F.J., Polvorinos, F., 1997. Atmospheric transportation of marihuana pollen from North Africa to the southwest of Europe. Atmospheric Environment 20, 3323–3328.

Cheng, M.-D., Hopke, P.K., Barrie, L., Rippe, A., Olson, M., Landsberger, S., 1993a. Qualitative determination of source regions of aerosol in Canadian high arctic. Environment Science and Technology 27, 2063–2071.

Cheng, M.-D., Hopke, P.K., Zeng, Y., 1993b. A receptor-oriented methodology for determining source regions of particulate sulfate at Dorset, Ontario. Journal of Geophysical Research 98, 16,839–16,849.

Chiapello, I., Bergametti, G., Chatenet, B., Bousquet, P., Dulac, F., Santos Soares, E., 1997. Origins of African dust transported over the northeastern tropical Atlantic. Journal of Geophysical Research 102, 13,701–13,709.

Chock, D.P., Kuo, Y.H., 1990. Comparison of wind-field models using the CAPTEX data. Journal of Applied Meteorology 29, 76–91.

Chock, D.P., Winkler, S.L., 1994a. A particle grid air quality modeling approach. 1. The dispersion aspect. Journal of Geophysical Research 99, 1019–1031.

Chock, D.P., Winkler, S.L., 1994b. A particle grid air quality modeling approach. 2. Coupling with chemistry. Journal of Geophysical Research 99, 1033–1041.

Clarke, J.F., Clark, T.L., Ching, J.K.S., Haagenson, P.L., Husar, R.B., Patterson, D.E., 1983. Assessment of model simulation of long-distance transport. Atmospheric Environment 12, 2449–2462.

Colin, J.L., Renard, D., Lescoat, V., Jaffrezo, J.L., Gros, M.J., Strauss, B., 1989. Relationship between rain and snow acidity and air mass trajectory in Eastern France. Atmospheric Environment 23, 1487–1498.

Comrie, A.C., 1994. Tracking ozone: air-mass trajectories and pollutant source regions influencing ozone in Pennsylvania forests. Annals of the Assocociation of American Geographers 84, 635–651.

D'Abreton, P.C., Tyson, P.D., 1996. Three-dimensional kinematic trajectory modelling of water vapour transport over Southern Africa. Water SA 22, 297–306.

Danielsen, E.F., 1961. Trajectories: isobaric, isentropic and actual. Journal of Meteorology 18, 479–486.

Davis, C.A., 1996. Potential vorticity. In: Schneider, S.H. (Ed.), Encyclopedia of Climate and Weather. Oxford University Press, Oxford.

De Leeuw, F.A.A.M., Van Rheineck Leyssius, H.J., Builtjes, P.J.H., 1990. Calculation of long term averaged ground level ozone concentrations. Atmospheric Environment 24A, 185–193.

Derwent, R.G., 1990. Evaluation of a number of chemical mechanisms for their application in models describing the formation of photochemical ozone in Europe. Atmospheric Environment 24A, 2615–2624.

Dorling, S.R., Davies, T.D., 1995. Extending cluster analysis—synoptic meteorology links to characterise chemical climates at six northwest European monitoring stations. Atmospheric Environment 29, 145–167.

Dorling, S.R., Davies, T.D., Pierce, C.E., 1992a. Cluster analysis: a technique for estimating the synoptic meteorological controls on air and precipitation chemistry—method and applications. Atmospheric Environment 26A, 2575–2581.

Dorling, S.R., Davies, T.D., Pierce, C.E., 1992b. Cluster analysis: a technique for estimating the synoptic meteorological controls on air and precipitation chemistry—results from Eskdalemuir, south Scotland. Atmospheric Environment 26A, 2583–2602.

Doty, K.G., Perkey, D.J., 1993. Sensitivity of trajectory calculations to the temporal frequency of wind data. Monthly Weather Review 121, 387–401.

Draxler, R.R., 1987. Sensitivity of a trajectory model to the spatial and temporal resolution of the meteorological data during CAPTEX. Journal of Climate and Applied Meteorology 26, 1577–1588.

Draxler, R.R., 1991. The accuracy of trajectories during ANATEX calculated using dynamic model analyses versus rawinsonde observations. Journal of Applied Meteorology 30, 1446–1467.

Draxler, R.R., 1996a. Boundary layer isentropic and kinematic trajectories during the August 1993 North Atlantic Regional Experiment Intensive. Journal of Geophysical Research 101, 29,255–29,268.

Draxler, R.R., 1996b. Trajectory optimization for balloon flight planning. Weather and Forecasting 11, 111–114.

Draxler, R.R., Dietz, R., Lagomarsino, R.J., Start, G., 1991. Across North America Tracer Experiment (ANATEX) sampling and analysis. Atmospheric Environment 25A, 2815–2836.

Draxler, R.R., McQueen, J.T., Stunder, B.J.B., 1994. An evaluation of air pollutant exposures due to the 1991 Kuwait oil fires using a Lagrangian model. Atmospheric Environment 28, 2197–2210.

Dutton, J.A., 1986. The Ceaseless Wind. An Introduction to the Theory of Atmospheric Motion. Dover, New York.

Eastman, J.L., Pielke, R.A., Lyons, W.A., 1995. Comparison of lake-breeze model simulations with tracer data. Journal of Applied Meteorology 34, 1398–1418.

Eder, B.K., Davis, J.M., Bloomfield, P., 1994. An automated classification scheme designed to better elucidate the dependence of ozone on meteorology. Journal of Applied Meteorology 33, 1182–1199.

Eliassen, A., Hov, Ø., Isaksen, I.S.A., Saltbones, J., Stordal, F., 1982. A Lagrangian long-range transport model with atmospheric boundary layer chemistry. Journal of Applied Meteorology 21, 1645–1661.

Fay, B., Glaab, H., Jacobsen, I., Schrodin, R., 1995. Evaluation of Eulerian and Lagrangian atmospheric transport models at the Deutscher Wetterdienst using ANATEX surface tracer data. Atmospheric Environment 29, 2485–2497.

Ferber, G.J., Heffter, J.L., Draxler, R.R., Lagomarsino, R.J., Thomas, F.L., Dietz, R.N., Benkovitz, C.M., 1986. Cross-Appalachian Tracer Experiment (CAPTEX 83). Final Rep. NOAA Techn. Memo. ERL ARL-142. Air Resources Laboratory, NOAA Environmental Research Laboratories. Silver Spring, Maryland 20910, p. 60.

Fernau, M.E., Samson, P.J., 1990a. Use of cluster analysis to define periods of similar meteorology and precipitation chemistry in Eastern North America. Part I: Transport patterns. Journal of Applied Meteorology 29, 735–750.

Fernau, M.E., Samson, P.J., 1990b. Use of cluster analysis to define periods of similar meteorology and precipitation chemistry in Eastern North America. Part II: Precipitation patterns and pollutant deposition. Journal of Applied Meteorology 29, 751–761.

Fisher, M., Lary, D.J., 1995. Lagrangian four-dimensional variational data assimilation of chemical species. Quarterly Journal of the Royal Meteorological Society 121, 1681–1704.

Flesch, T.K., 1996. The footprint for flux measurements, from backward Lagrangian stochastic models. Boundary-Layer Meteorology 78, 399–404.

Flesch, T.K., Wilson, J.D., Yee, E., 1995. Backward-time Lagrangian stochastic dispersion models, and their application to estimate gaseous emissions. Journal of Applied Meteorology 34, 1320–1332.

Fuelberg, H.E., Loring, R.O., Jr, Watson, M.V., Sinha, M.C., Pickering, K.E., Thompson, A.M., Sachse, G.W., Blake, D.R., Schoeberl, M.R., 1996. TRACE A trajectory intercomparison. 2. Isentropic and kinematic methods. Journal of Geophysical Research 101, 23,927–23,939.

Gao, N., Cheng, M.-D., Hopke, P.K., 1993. Potential source contribution function analysis and source apportionment of sulfur species measured at Rubidoux, CA during the Southern California Air Quality Study, 1987. Analytica Chimica Acta 277, 369–380.

Goodin, W.R., McRae, G., Seinfeld, J.H., 1980. An objective analysis technique for constructing three-dimensional urban-scale wind fields. Journal of Applied Meteorology 19, 98–108.

Grell, G.A., Dudhia, J., Stauffer, D.R., 1995. A description of the fifth-generation Penn State/NCAR mesoscale model (MM5). NCAR Technical Note, NCAR/TN-398 + STR, p. 122.

Haagenson, P.L., Gao, K., Kuo, Y.-H., 1990. Evaluation of meteorological analyses, simulations, and long-range transport using ANATEX surface tracer data. Journal of Applied Meteorology 29, 1268–1283.

Haagenson, P.L., Kuo, Y.H., Skumanich, M., Seaman, N.L., 1987. Tracer verification of trajectory models. Journal of Climate and Applied Meteorology 26, 410–426.

Hanna, S.R., 1982. Applications in air pollution modeling. In: Nieuwstadt, F.T.M., van Dop, H.D. (Eds.), Atmospheric Turbulence and Air Pollution Modelling. Reidel, Dordrecht, Holland.

Harris, J.M., 1992. An analysis of 5-day midtropospheric flow patterns for the South Pole: 1985–1989. Tellus 44B, 409–421.

Harris, J.M., Kahl, J.D., 1990. A descriptive atmospheric transport climatology for the Mauna Loa Observatory, using clustered trajectories. Journal of Geophysical Research 95, 13,651–13,667.

Harris, J.M., Kahl, J.D.W., 1994. Analysis of 10-day isentropic flow patterns for Barrow, Alaska: 1985–1992. Journal of Geophysical Research 99, 25,845–25,855.

Heffter, J.L., 1980. Air Resources Laboratories Atmospheric Transport and Dispersion Model (ARL-ATAD). NOAA Techn. Memo. ERL ARL-81. NOAA Environmental Research Laboratories. Boulder, Colorado, USA, p. 17.

Heffter, J.L., 1983. Branching Atmospheric Trajectory (BAT) Model. NOAA Techn. Memo. ERL ARL-121, Air Resources Laboratory. Silver Springs, Maryland, USA, p. 19.

Heffter, J.L., Stunder, B.J.B., 1993. Volcanic ash forecast transport and dispersion (VAFTAD) model. Weather and Forecasting 8, 533–541.

Heffter, J.L., Stunder, B.J.B., Rolph, G.D., 1990. Long-range forecast trajectories of volcanic ash from Redoubt Volcano eruptions. Bulletin of the American Meteorological Society 71, 1731–1738.

Henderson, R.G., Weingartner, K., 1982. Trajectory analysis of MAP3S precipitation chemistry data at Ithaca, New York. Atmospheric Environment 16, 1657–1665.

Hertel, O., Christensen, J., Runge, E.H., Asman, W.A.H., Berkowicz, R., Hovmand, M.F., Hov, Ø., 1995. Development and testing of a new variable scale air pollution model—ACDEP. Atmospheric Environment 29, 1267–1290.

Henmi, T., 1980. Long-range transport of SO_2 and sulfate and its application to the eastern United States. Journal of Geophysical Research 85, 4436–4442.

Hoecker, W.H., 1977. Accuracy of various techniques for estimating boundary-layer trajectories. Journal of Applied Meteorology 16, 374–383.

Hopke, P.K., Gao, N., Cheng, M.-D., 1993. Combining chemical and meteorological data to infer source areas of airborne pollutants. Chemom. Intell. Lab. Syst. 19, 187–199.

Jäger, A., 1992. Isentrope Trajektorien und ihre Anwendung auf das Konzept der potentiellen Vorticity bei orographisch induzierten Lee-Zyklogenesen. Diploma Thesis. University of Innsbruck, Austria.

Kahl, J.D., 1993. A cautionary note on the use of air trajectories in interpreting atmospheric chemistry measurements. Atmospheric Environment 27A, 3037–3038.

Kahl, J.D.W., 1996. On the prediction of trajectory model error. Atmospheric Environment 30, 2945–2957.

Kahl, J.D., Harris, J.M., Herbert, G.A., Olson, M.P., 1989a. Intercomparison of long-range trajectory models applied to arctic haze. Proceedings of the 17th NATO/CCMS ITM on Air Pollution Model and its Applications. Plenum Press, New York, pp. 175–185.

Kahl, J.D., Harris, J.M., Herbert, G.A., Olson, M.P., 1989b. Intercomparison of three long-range trajectory models applied to Arctic haze. Tellus 41B, 524–536.

Kahl, J.D., Liu, D., White, W.H., Macias, E.S., Vasconcelos, L., 1997. The relationship between atmospheric transport and the particle scattering coefficient at the Grand Canyon. Journal of Air and Waste Management Association 47, 419–425.

Kahl, J.D., Samson, P.J., 1986. Uncertainty in trajectory calculations due to low resolution meteorological data. Journal of Climate and Applied Meteorology 25, 1816–1831.

Kahl, J.D., Samson, P.J., 1988a. Trajectory sensitivity to rawinsonde data resolution. Atmospheric Environment 22, 1291–1299.

Kahl, J.D., Samson, P.J., 1988b. Uncertainty in estimating boundary-layer transport during highly convective conditions. Journal of Applied Meteorology 27, 1024–1035.

Kahl, J.D., Schnell, R.C., Sheridan, P.J., Zak, B.D., Church, H.W., Mason, A., Heffter, J.L., Harris, J.M., 1991. Predicting atmospheric debris transport in real-time using a trajectory forecast model. Atmospheric Environment 25A, 1705–1713.

Kalkstein, L.S., Tan, G., Skindlov, J.A., 1987. An evaluation of three clustering procedures for use in synoptic climatological classification. Journal of Climate and Applied Meteorology 26, 717–730.

Klug, W., Graziani, G., Grippa, G., Pierce, D., Tassone, C.W., 1992. Evaluation of Long Range Atmospheric Transport Models Using Environmental Radioactivity Data from the Chernobyl Release. Elsevier, Amsterdam.

Knudsen, B.M., Carver, G.D., 1994. Accuracy of the isentropic trajectories calculated for the EASOE campaign. Geophysical Research Letters 21, 1199–1202.

Knudsen, B.M., Rosen, J.M., Kjome, N.T., Whitten, A.T., 1996. Comparison of analyzed stratospheric temperatures and calculated trajectories with long-duration balloon data. Journal of Geophysical Research 101, 19,137–19,145.

Koffi, N.E., Nodop, K., Benech, B., 1997a. Constant volume balloon model used to derive tracer plume trajectories (ETEX experiment first release). In: Nodop, K. (Ed.), ETEX Symposium on Long-Range Atmospheric Transport, Model Verification and Emergency Response. European Commission EUR 17346, pp. 75–78.

Koffi, N.E., Nodop, K., Benech, B., 1997b. Constant volume balloon model used to derive tracer plume trajectories (ETEX experiment second release). In: Nodop, K. (Ed.), ETEX Symposium on Long-Range Atmospheric Transport, Model Verification and Emergency Response. European Commission EUR 17346, pp. 79–82.

Kolb, H., Seibert, P., Zwatz-Meise, V., Mahringer, G., 1989. Comparison of trajectories calculated during and after the Chernobyl accident. In: Evaluation of atmospheric dispersion models applied to the release from Chernobyl. Österreichische Beiträge zu Meteorologie und Geophysik 1, 61–69.

Kuo, Y.-H., Skumanich, M., Haagenson, P.L., Chang, J.S., 1985. The accuracy of trajectory models as revealed by the observing system simulation experiments. Monthly Weather Review 113, 1852–1867.

Lamb, B.K., Lorenzen, A., Shair, F.H., 1978a. Atmospheric dispersion and transport within coastal regions—part I. Tracer study of power plant emissions from the Oxnard plain. Atmospheric Environment 12, 2089–2100.

Lamb, B.K., Shair, F.H., Smith, T.B., 1978b. Atmospheric dispersion and transport within coastal regions—part II. Tracer study of industrial emissions in the California delta region. Atmospheric Environment 12, 2101–2118.

Legg, B.J., Raupach, M.R., 1982. Markov-chain simulation of particle dispersion in inhomogeneous flows: the mean drift velocity induced by a gradient in Eulerian velocity variance. Boundary-Layer Meteorology 24, 3–13.

Lorimer, G.S., 1986. The kernel method for air quality modelling—I. Mathematical foundation. Atmospheric Environment 20, 1447–1452.

Luhar, A.K., Hibberd, M.F., Hurley, P.J., 1996. Comparison of closure schemes used to specify the velocity PDF in Lagrangian stochastic dispersion models for convective conditions. Atmospheric Environment 30, 1407–1418.

Ludwig, F.L., Livingston, J.M., Endlich, R.M., 1991. Use of mass conservation and critical dividing streamline concepts for efficient objective analysis of wind fields in complex terrain. Journal of Applied Meteorology 30, 1490–1499.

Lyons, W.A., Pielke, R.A., Tremback, C.J., Walko, R.L., Moon, D.A., Keen, C.S., 1995. Modeling impacts of mesoscale vertical motions upon coastal zone air pollution dispersion. Atmospheric Environment 29, 283–301.

Martin, D., Bergametti, G., Strauss, B., 1990. On the use of the synoptic vertical velocity in trajectory model: validation by geochemical tracers. Atmospheric Environment 24A, 2059–2069.

Martin, D., Mithieux, C., Strauss, B., 1987. On the use of the synoptic vertical wind component in a transport trajectory model. Atmospheric Environment 21, 45–52.

Maryon, R.H., Buckland, A.T., 1994. Diffusion in a Lagrangian multiple particle model: a sensitivity study. Atmospheric Environment 28, 2019–2038.

Maryon, R.H., Heasman, C.C., 1988. The accuracy of plume trajectories forecast using the U.K. meteorological office operational forecasting models and their sensitivity to calculation schemes. Atmospheric Environment 22, 259–272.

Mathur, R., Peters, L.K., 1990. Adjustment of wind fields for application in air pollution modeling. Atmospheric Environment 24A, 1095–1106.

McNider, R.T., Moran, M.D., Pielke, R.A., 1988. Influence of diurnal and inertial boundary layer oscillations on long-range dispersion. Atmospheric Environment 22, 2445–2462.

McQueen, J.T., Draxler, R.R., 1994. Evaluation of model back trajectories of the Kuwait oil fires smoke plume using digital satellite data. Atmospheric Environment 28, 2159–2174.

Merrill, J.T., Bleck, R., Avila, L., 1985. Modeling atmospheric transport to the Marshall islands. Journal of Geophysical Research 90, 12,927–12,936.

Merrill, J.T., Bleck, R., Boudra, D., 1986. Techniques of Lagrangian trajectory analysis in isentropic coordinates. Monthly Weather Review 114, 571–581.

Miller, J.M., 1981. A five-year climatology of back trajectories from the Mauna Loa observatory, Hawaii. Atmospheric Environment 15, 1553–1558.

Miller, J.M., 1987. The use of back air trajectories in interpreting atmospheric chemistry data: a review and bibliography. NOAA Technical Memo. ERL ARL-155. Air Resources Laboratory, NOAA Environmental Research Laboratories. Silver Spring, Maryland, USA, p. 60.

Miller, J.M., Moody, J.L., Harris, J.M., Gaudry, A., 1993. A 10-year trajectory flow climatology for Amsterdam island, 1980–1989. Atmospheric Environment 27A, 1909–1916.

Moody, J.L., Galloway, J.N., 1988. Quantifying the relationship between atmospheric transport and the chemical composition of precipitation on Bermuda. Tellus 40B, 463–479.

Moody, J.L., Oltmans, S.J., Levy II, H., Merrill, J.T., 1995. Transport climatology of tropospheric ozone: Bermuda, 1988–1991. Journal of Geophysical Research 100, 7179–7194.

Moody, J.L., Samson, P.J., 1989. The influence of atmospheric transport on precipitation chemistry at two sites in the midwestern United States. Atmospheric Environment 23, 2117–2132.

Moran, M.D., Pielke, R.A., 1996. Evaluation of a mesoscale atmospheric dispersion modeling system with observations from the 1980 Great Plains mesoscale tracer field experiment. Part II: Dispersion simulations. Journal of Applied Meteorology 35, 308–329.

Mosca, S., Graziani, G., Klug, W., Bellasio, R., Bianconi, R., 1997. ATMES-II – Evaluation of Long-Range Dispersion Models Using 1st ETEX Release Data, Vol. I (in press).

Munn, R.E., Likens, G.E., Weisman, B., Hornbeck, J.W., Martin, C.W., Bormann, F.H., 1984. A meteorological analysis of the precipitation chemistry event samples at Hubbard Brook (N.H.). Atmospheric Environment 18, 2775–2779.

Nguyen, K.C., Noonan, J.A., Galbally, I.E., Physick, W.L., 1997. Predictions of plume dispersion in complex terrain: Eulerian versus Lagrangian models. Atmospheric Environment 31, 947–958.

Pack, D.H., Ferber, G.J., Heffter, J.L., Telegadas, K., Angell, J.K., Hoecker, W.H., Machta, L., 1978. Meteorology of long-range transport. Atmospheric Environment 12, 425–444.

Peters, L.K., Berkowicz, C.M., Carmichael, G.R., Easter, R.C., Fairweather, G., Ghan, S.J., Hales, J.M., Leung, L.R., Pennell, W.R., Potra, F.A., Saylor, R.D., Tsang, T.T., 1995. The current state and future direction of Eulerian models in simulating the tropospheric chemistry and transport of trace species: a review. Atmospheric Environment 29, 189–222.

Petersen, R.A., Uccellini, L.W., 1979. The computation of isentropic atmospheric trajectories using a "Discrete Model" formulation. Monthly Weather Review 107, 566–574.

Petterssen, S., 1940. Weather Analysis and Forecasting. McGraw–Hill, New York, pp. 221–223.

Pflüger, U., Roos, M., Jacobsen, I., 1990. Trajektorienberechnungen auf Basis des neuen Wettervorhersagesystems des Deutschen Wetterdienstes und ihre Anwendung für die Ausbreitungsrechnung. Deutscher Wetterdienst.

Pickering, K.E., Thompson, A.M., McNamara, D.P., Schoeberl, M.R., 1994. An intercomparison of isentropic trajectories over the South Atlantic. Monthly Weather Review 122, 864–879.

Pickering, K.E., Thompson, A.M., McNamara, D.P., Schoeberl, M.R., Fuelberg, H.E., Loring, R.O., Jr., Watson, M.V., Fakhruzzaman, K., Bachmeier, A.S., 1996. TRACE A trajectory intercomparison. 1. Effects of different input analyses. Journal of Geophysical Research 101, 23,903–23,925.

Pielke, R.A., Cotton, W.R., Walko, R.L, Trembach, C.J., Lyons, W.A., Grasso, L.D., Nicholls, M.E., Moran, M.D., Wesely, D.A., Lee, T.J., Copeland, J.H., 1992. A comprehensive meteorological modeling system – RAMS. Meteorology Atmospheric Physics 49, 69–91.

Poirot, R.L., Wishinski, P.R., 1986. Visibility, sulfate and air mass history associated with the summertime aerosol in Northern Vermont. Atmospheric Environment 20, 1457–1469.

Rao, S.T., Pleim, J., Czapaski, J., 1983. A comparative study of two trajectory models of long-range transport. Journal of Air Pollution Control Association 33, 32–41.

Raynor, G.S., Hayes, J.V., Lewis, D.M., 1983. Testing of the Air Resources Laboratories trajectory model on cases of pollen wet deposition after long-distance transport from known source regions. Atmospheric Environment 17, 213–220.

Reiff, J., Forbes, G.S., Spieksma, F.T.M., Reynders, J.J., 1986. African dust reaching northwestern Europe: a case study to verify trajectory calculations. Journal of Climate and Applied Meteorology 25, 1543–1567.

Reisinger, L.M., Mueller, S.F., 1983. Comparisons of tetroon and computed trajectories. Journal of Climate and Applied Meteorology 22, 664–672.

Rodean, H., 1996. Stochastic Lagrangian models of turbulent diffusion. Meteorological Monographs 26 (48). American Meteorological Society, Boston, USA.

Rolph, G.D., Draxler, R.R., 1990. Sensitivity of three-dimensional trajectories to the spatial and temporal densities of the wind field. Journal of Applied Meteorology 29, 1043–1054.

Ross, D.G., Smith, I.N., Manins, P.C., Fox, D.G., 1988. Diagnostic wind field modeling for complex terrain: model development and testing. Journal of Applied Meteorology 27, 785–796.

Sardeshmukh, P.D., Liebmann, B., 1993. An assessment of low-frequency variability in the tropics as indicated by some proxies of tropical convection. Journal of Climate 6, 569–575.

Scire, J., Insley, E., Yamartino, R., 1990. Model formulation and user's guide for the CALMET meteorological model. Report No. A025-1, prepared for the State of California Air Resources Board.

Scheele, M.P., Siegmund, P.C., Velthoven, P.F.J., 1996. Sensitivity of trajectories to data resolution and its dependence on the starting point: in or outside a tropopause fold. Meteorological Applications 3, 267–273.

Schlünzen, K.H., 1994. Mesoscale modeling in complex terrain—an overview on the German nonhydrostatic models. Beiträge zur Physik der Atmosphäre 67, 243–253.

Seibert, P., 1993. Convergence and accuracy of numerical methods for trajectory calculations. Journal of Applied Meteorology 32, 558–566.

Seibert, P., 1997. Inverse dispersion modelling based on trajectory-derived source-receptor relationships. Proceedings of the 22nd International Technical Meeting on Air Pollution Modelling and its Applications, Clermont-Ferrand.

Seibert, P., Kromp-Kolb, H., Baltensperger, U., Jost, D.T., Schwikowski, M., 1994a. Trajectory analysis of high-alpine air pollution data. In: Gryning, S.-E., Millan, M.M. (Eds.), Air Pollution Modelling and its Application X. Plenum Press, New York, pp. 595–596.

Seibert, P., Kromp-Kolb, H., Baltensperger, U., Jost, D.T., Schwikowski, M., Kasper, A., Puxbaum, H., 1994b. Trajectory analysis of aerosol measurements at high alpine sites. In: Borrell, P.M., Borrell, P., Cvitaš, T., Seiler, W. (Eds.), Transport and Transformation of Pollutants in the Troposphere. Academic Publishing, Den Haag, pp. 689–693.

Sherman, C.A., 1978. A mass-consistent model for wind fields over complex terrain. Journal of Applied Meteorology 17, 312–319.

Shi, B., Kahl, J.D., Christidis, Z.D., Samson, P.J., 1990. Simulation of the three-dimensional distribution of tracer during the Cross-Appalachian Tracer Experiment. Journal of Geophysical Research 95, 3693–3703.

Sirois, A., Bottenheim, J.W., 1995. Use of backward trajectories to interpret the 5-year record of PAN and O_3 ambient air concentrations at Kejimkujik National Park, Nova Scotia. Journal of Geophysical Research 100, 2867–2881.

Sparling, L.C., Schoeberl, M.R., Douglass, A.R., Weaver, C.J., Newman, P.A., Lait, L.R., 1995. Trajectory modeling of emissions from lower stratospheric aircraft. Journal of Geophysical Research 100, 1427–1438.

Steinacker, R., 1984. Airmass and frontal movement around the Alps. Rivista di Meteorologia Aeronautica 44, 85–93.

Stevenson, D.S., Collins, W.J., Johnson, C.E., Derwent, R.G., 1997. The impact of aircraft nitrogen oxide emissions on tropospheric ozone studied with a 3D Lagrangian model including fully diurnal chemistry. Atmospheric Environment 31, 1837–1850.

Stocker, R.A., Pielke, R.A., Verdon, A.J., Snow, J.T., 1990. Characteristics of plume releases as depicted by balloon launchings and model simulations. Journal of Applied Meteorology 29, 53–62.

Stohl, A., 1996a. On the use of trajectories for establishing source-receptor relationships of air pollutants. Ph.D. Thesis. University of Vienna.

Stohl, A., 1996b. Trajectory statistics—a new method to establish source–receptor relationships of air pollutants and its application to the transport of particulate sulfate in Europe. Atmospheric Environment 30, 579–587.

Stohl, A., Baumann, K., Wotawa, G., Langer, M., Neininger, B., Piringer, M., Formayer, H., 1997. Diagnostic downscaling of large scale wind fields to compute local scale trajectories. Journal of Applied Meteorology 36, 931–942.

Stohl, A., Kromp-Kolb, H., 1994a. Origin of ozone in Vienna and surroundings, Austria. Atmospheric Environment 28, 1255–1266.

Stohl, A., Kromp-Kolb, H., 1994b. Frequency of ozone formation in the plume of Vienna. In: Baldasano, J.M., Brebbia, C.A., Power, H., Zannetti, P. (Eds.), Air Pollution 2, Vol. 2—Pollution Control and Monitoring. Computational Mechanics Publications, Southampton, Boston, UK, pp. 449–456.

Stohl, A., Scheifinger, H., 1994. A weather pattern classification by trajectory clustering. Meteorologische Zeitschrift N.F. 6, 333–336.

Stohl, A., Seibert, P., 1997. Accuracy of trajectories as determined from the conservation of meteorological tracers. Quarterly Journal of the Royal Meteorological Society, in press.

Stohl, A., Wotawa, G., 1995. A method for computing single trajectories representing boundary layer transport. Atmospheric Environment 29, 3235–3239.

Stohl, A., Wotawa, G., Seibert, P., Kromp-Kolb, H., 1995. Interpolation errors in wind fields as a function of spatial and temporal resolution and their impact on different types of kinematic trajectories. Journal of Applied Meteorology 34, 2149–2165.

Stunder, B.J.B., 1996. An assessment of the quality of forecast trajectories. Journal of Applied Meteorology 35, 1319–1331.

Sutton, R., 1994. Lagrangian flow in the middle atmosphere. Quarterly Journal of the Royal Meteorological Society 120, 1299–1321.

Tajima, T., Nakamura, T., Kurokawa, K., 1997. Experimental observations of 3-D Lagrangian motion in a steady baroclinic wave. Journal of the Meteorological Society of Japan 75, 101–109.

Thomson, D.J., 1984. Random walk modelling of diffusion in inhomogeneous turbulence. Quarterly Journal of the Royal Meteorological Society 110, 1107–1120.

Thomson, D.J., 1987. Criteria for the selection of stochastic models of particle trajectories in turbulent flows. Journal of Fluid Mechanics 180, 529–556.

Thomson, D.J., Montgomery, M.R., 1994. Reflection boundary conditions for random walk models of dispersion in non-Gaussian turbulence. Atmospheric Environment 28, 1981–1987.

Tyson, P.D., Garstang, M., Swap, R., 1996. Large-scale recirculation of air over southern Africa. Journal of Applied Meteorology 35, 2218–2236.

Uliasz, M., 1994. Lagrangian particle dispersion modeling in mesoscale applications. In: Zannetti, P. (Ed.), Environmental Modeling, Vol. II. Computational Mechanics Publications, Southampton, UK, pp. 71–101.

Uliasz, M., Stocker, R.A., Pielke, R.A., 1997. Regional modeling of air pollution transport in the southwestern United States. To be published in: Zannetti, P. (Ed.), Environmental Modeling, Vol. III. Computational Mechanics Publications, Southampton, U.K.

Vasconcelos, L.A.P., Kahl, J.D.W., Liu, D., Macias, E.S., White, W.H., 1996a. A tracer calibration of back trajectory analysis at the Grand Canyon. Journal of Geophysical Research 101, 19329–19335.

Vasconcelos, L.A.P., Kahl, J.D.W., Liu, D., Macias, E.S., White, W.H., 1996b. Spatial resolution of a transport inversion technique. Journal of Geophysical Research 101, 19,337–19,342.

Virkkula, A., Mäkinen, M., Hillamo, R., Stohl, A., 1995. Atmospheric aerosol in the Finnish Arctic: particle number concentrations, chemical characteristics, and source analysis. Water, Air and Soil Pollution 85, 1997–2002.

Walmsley, J.L., Mailhot, J., 1983. On the numerical accuracy of trajectory models for long-range transport of atmospheric pollutants. Atmos.-Ocean 21, 14–39.

Warner, T.T., Fizz, R.R., Seaman, N.L., 1983. A comparison of two types of atmospheric transport models—use of observed winds versus dynamically predicted winds. Journal of Climate and Applied Meteorology 22, 394–406.

Waugh, D.W., Plumb, R.A., 1994. Contour advection with surgery: a technique for investigating finescale structures in tracer transport. Journal of Atmospheric Science 51, 530–540.

Wetzel, M., Borys, R., Lowenthal, D., Brown, S., 1995. Meteorological support to the Earthwinds Transglobal Balloon project. Bulletin of the American Meteorological Society 76, 477–487.

White, W.H., Macias, E.S., Kahl, J.D., Samson, P.J., Molenar, J.V., Malm, W.C., 1994. On the potential of regional-scale emissions zoning as an air quality management tool for the Grand Canyon. Atmospheric Environment 28, 1035–1045.

Wilson, J.D., Flesch, T.K., 1993. Flow boundaries in random-flight dispersion models: enforcing the well-mixed condition. Journal of Applied Meteorology 32, 1695–1707.

Wilson, J.D., Legg, B.J., Thomson, D.J., 1983. Calculation of particle trajectories in the presence of a gradient in turbulent-velocity scale. Boundary-Layer Meteorology 27, 163–169.

Wilson, J.D., Sawford, B.L., 1996. Review of Lagrangian stochastic models for trajectories in the turbulent atmosphere. Boundary-Layer Meteorology 78, 191–210.

Zeng, Y., Hopke, P.K., 1989. A study of the sources of acid precipitation in Ontario, Canada. Atmospheric Environment 23, 1499–1509.

Zannetti, P., 1992. Particle modeling and its application for simulating air pollution phenomena. In: Melli, P., Zannetti, P. (Eds.), Environmental Modelling. Computational Mechanics Publications, Southampton, UK, pp. 211–241.